

UNCLASSIFIED

AD 407 305

DEFENSE DOCUMENTATION CENTER

FOR

SCIENTIFIC AND TECHNICAL INFORMATION

CAMERON STATION, ALEXANDRIA, VIRGINIA



UNCLASSIFIED

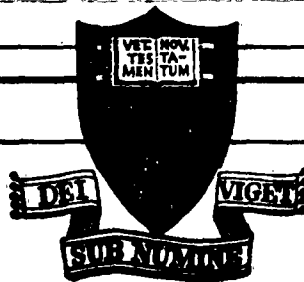
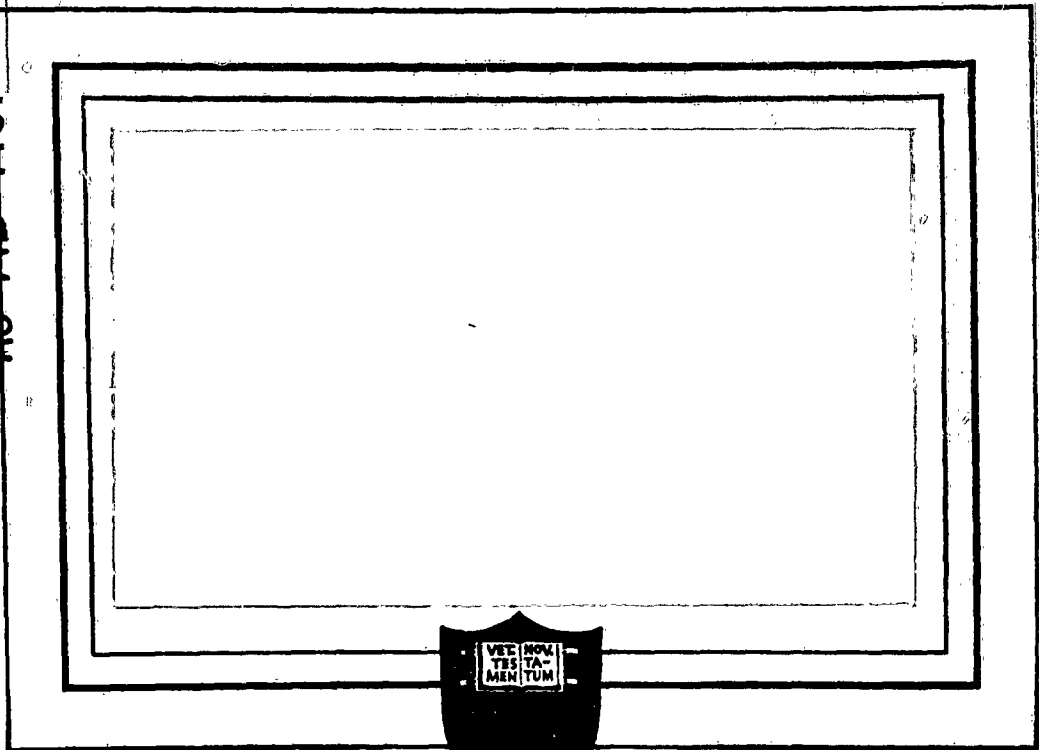
NOTICE: When government or other drawings, specifications or other data are used for any purpose other than in connection with a definitely related government procurement operation, the U. S. Government thereby incurs no responsibility, nor any obligation whatsoever; and the fact that the Government may have formulated, furnished, or in any way supplied the said drawings, specifications, or other data is not to be regarded by implication or otherwise as in any manner licensing the holder or any other person or corporation, or conveying any rights or permission to manufacture, use or sell any patented invention that may in any way be related thereto.

63-4-1

CATALOGED BY DDC

AS AD No 407305

407 305



DDC
RECEIVED
JUN 22 1963
TISIA B

PRINCETON UNIVERSITY

Princeton University
ONR Contract Nonr 1858(27)
NR-014-203

Technical Report No. 15

VIBRATION - ROTATION SPECTRA OF CH_4 AND CD_4
IMPURITIES IN XENON, KRYPTON AND ARGON CRYSTALS

by

A. Cabana, D.F. Hornig and G.B. Savitsky
Frick Chemical Laboratory, Princeton University
Princeton, N.J.

June 1963

Vibration - Rotation Spectra of CH_4 and CD_4
Impurities in Xenon, Krypton and Argon Crystals

by

A. Cabana, D.F. Hornig and G.B. Savitsky*

Frick Chemical Laboratory, Princeton University
Princeton, N.J.

Abstract

The infrared spectra of CH_4 and CD_4 , present as substitutional impurities in crystals of argon, krypton and xenon, were studied at temperatures ranging from 5 to 40°K.

Both ν_3 and ν_4 of CH_4 in xenon showed a simple four line pattern which is consistent with that expected for a slightly hindered rotor. In krypton and argon a fifth line appeared on ν_3 , as expected from King's theoretical calculations for a tetrahedral rotor in an octahedral field. In addition, argon showed absorption due to pairs or higher aggregates of CH_4 molecules.

The rotational spectrum of CD_4 is much more highly perturbed. Detailed assignments to hindered rotational levels could not be made but the general features are in accord with King's model.

The frequencies of the CH_4 and CD_4 absorption bands increase steadily in going from xenon to krypton to argon. This can be accounted for by the decrease in the sizes of the cavities occupied, with corresponding larger repulsive interactions between the CH_4 or CD_4 and the host atoms.

*Present address: Dept. of Chemistry, U. of California, Davis, Calif.

Introduction

The question of molecular rotation in solids is an old one; it has been supposed at one time or another that a wide variety of molecules rotated freely in at least one crystal phase, but the list has gradually dwindled and at the present time the evidence for quantized rotation is only strong for crystalline hydrogen. For example, it has been shown recently that the energy barrier to rotation is fairly high in all of the crystalline phases of CH_4 and CD_4 ¹.

1. G.B. Savitsky and D.F. Hornig, J. Chem. Phys., 36, 2634 (1962).

Rotational fine structure has been reported in the infrared spectra of a number of small molecules trapped in noble gas matrices. In many cases the spectra are complicated and alternative origins for the fine structure are possible so that the identification of the fine structure with rotational transitions is somewhat ambiguous. For example, the fine structure of NH_3 in solid nitrogen which was originally ascribed to rotation² was later shown to originate in pure vibrational spectra of poly-

2. D.E. Milligan, R.M. Hexter and K. Dressler, J. Chem. Phys., 34, 1009 (1961):

meric ammonia molecules³. Water molecules suspended in argon also show

3. G.C. Pimentel, M.O. Bulanin and M. Van Thiel, J. Chem. Phys., 36, 500 (1962).

extensive fine structure which correlates well with the spectrum of gaseous H_2O , and on this basis Redington and Milligan⁴ have concluded that water

4. R.L. Redington and D.E. Milligan, J. Chem. Phys., 37, 2162 (1962).

molecules rotate freely in crystalline argon. This result is unexpected since the solute molecules are larger than the available cavities, even on substitutional sites (See Tables I and II). Similarly, hydrogen chloride has been reported to rotate in solid argon, although it too has a larger van der Waal's radius than a substitutional hole in the face centered cubic lattice of argon⁵. It might, moreover, have been expected

5. Schoen, Mann, Knobler and White, J. Chem. Phys., 37, 1146 (1962).

that the polarity of HCl would have produced strong maxima and minima in the potential field.

It seemed important, therefore, to study a system in which the molecule fitted the crystal lattice without much distortion, which had a simple gas phase spectrum and for which the perturbation by the crystal lattice could be understood, at least qualitatively and perhaps quantitatively. These conditions are met by the system CH₄ (or CD₄) in krypton or xenon.

Methane and krypton are known to form solid solutions at all concentrations⁶, indicating that there is no tendency for the methane molecules

6. J.G. Aston, J. Chem. Phys. Solids, 18, 62 (1961).

to form clusters in the matrix. Furthermore, since CH₄ fits almost exactly into a substitutional hole of crystalline xenon, which is bigger than the corresponding hole in solid krypton (See Tables I and II), we may assume with confidence that methane and xenon will also form solid solutions. The nearly spherical shape of methane (symmetry T_d) will tend to make its energy of interaction with the noble gas atoms less dependent upon

its orientation in the matrix (symmetry O_h), making it a particularly favorable case in which to observe rotation. Finally, the theory of the hindered rotational levels of a spherical top in an octahedral field has been worked out in considerable detail⁷. For all of these reasons, we

7. H.F. King, Ph.D. Thesis, Princeton University, 1960.

undertook to study the infrared spectra of dilute solid solutions of CH_4 and CD_4 in crystalline argon, krypton and xenon.

EXPERIMENTAL

The low temperature cell used in this work has been described previously¹ and was capable of achieving a certain amount of temperature control. The copper sample holder was connected to the helium pot through a four inch long stainless steel tube which extended half-way into the body of the pot, its upper end being open. When the pot was completely filled, the liquid helium came in direct contact with the sample holder, yielding the lowest possible temperature. When the pot was only half filled, the helium in the tube boiled off very rapidly, so that the heat flow from the sample to the pot was largely restricted to conduction by the walls of the stainless steel tube. In this way, without additional heating a temperature difference of about 11°K could be established between the pot and the silver chloride backing plate.

The gas mixtures were prepared by introducing accurately known amounts of methane and noble gases into a 600 c.c. bulb. A part of the gas mixing apparatus was then heated to about 100°C for a few hours in order to create convection currents and ensure complete mixing. All compounds were research grade and were used without further purification.

The solid samples were prepared by spraying the gaseous mixtures on a silver chloride plate cooled by liquid helium. Slow deposition gave glassy films which, in some extreme cases, could not be annealed. Fast deposition, on the contrary, gave crystalline samples which required very little annealing. Scattered light was greatly reduced when the deposition was made at about 20°K.

The temperatures were measured with a carbon resistor embedded in the silver chloride plate and calibrated at the temperatures of boiling helium, the triple point of nitrogen, boiling nitrogen and room temperatures. The accuracy is believed to be $\pm 1^\circ\text{K}$ at the lowest temperature and always better than $\pm 5^\circ\text{K}$. A temperature rise of about 1°K was detected on the AgCl plate when the full energy from the globar fell on the sample. This heating effect was greatly reduced when an appropriate filter was placed between the source and the sample.

The spectra were recorded on a Perkin-Elmer model 112 G spectrometer, the spectral slit width of which is of the order of 0.5 cm^{-1} to 0.9 cm^{-1} in the regions of present interest under the conditions used. It was calibrated using the I.U.P.A.C. data⁸.

8. Tables of Wavenumbers for the Calibration of Infra-Red Spectrometers (Butterworths, Washington (1961)).

DISCUSSION OF THE SPECTRA

Typical spectra of methane and deuteromethane in noble gas crystals are presented in Figures 1 to 3 and 5 and 6 respectively. Figures 4 and 7 summarize the results obtained for CH_4 and CD_4 respectively.

Fine structure is observed on both the ν_3 (stretching) and ν_4 (bending)

bands which might be explained in several ways, namely:

- a) the solute molecules are not distributed randomly in the matrix but form pairs or higher order clusters,
- b) the solute molecules occupy various types of sites in the face-centered cubic lattice,
- c) the solute molecules lie at crystal imperfections and surface sites,
- d) the solute molecules occupy low symmetry sites or lose some of their symmetry elements,
- e) the solute molecules undergo free or hindered rotation.

One of these, or a combination of these causes, should be responsible for our findings. Each of these possibilities will therefore be reviewed in detail.

Formation of Clusters

Behringer⁹ has computed the probability for a molecule, in a face-

9. R.E. Behringer, J. Chem. Phys., 29, 537 (1958).

centered cubic lattice containing two types of molecules randomly distributed over the sites, to have a nearest neighbor of its own kind. According to these calculations, some 5 % of the solute molecules are paired when the concentration is 0.5 % and some 25 % at a concentration of 5 %. Nevertheless, no significant differences were found in the spectra of xenon solutions in the concentration range 0.5 to 5 % (see Figures 1-a,c,d), implying that no pairs were formed at any of these concentrations. This implies in turn that the molecules of methane are not randomly distributed over the sites in xenon but that the distribution is

such as to avoid formation of pairs. The absence of pairs is confirmed by comparison of the xenon spectra with the spectra of a 0.2 % argon solution (Figures 3-a,b,c,d).

When the temperature of a solid argon solution, prepared at 20°K is raised to about 30°K in the annealing process, a new broad band with some structure appears on the low frequency side of the main features. It is seen to grow in intensity as a function of time when the temperature is kept high enough ($\sim 30^{\circ}\text{K}$). The only possible explanation for the appearance of this band is that at a sufficiently high temperature the solute molecules diffuse through the argon crystal to form clusters. Two factors are probably responsible for the behavior of this mixed crystal, the first being a loss of rigidity of the argon crystal which seems to occur at a much lower temperature than in krypton or xenon, the second one being that the methane molecules are much too big to fit in any cavity of the argon crystal so that the crystal structure may be distorted and consequently less stable in their vicinity.

We may then conclude that the formation of clusters cannot account for the fine structure found in xenon or krypton crystals. Moreover, even in solid argon solutions, it seems that clusters are responsible for the extra bands which appeared after diffusion took place, but not for the fine structure observed before diffusion (Figure 3-a).

Different Trapping Sites.

A knowledge of the van der Waals radii and crystal parameters of the noble gas enables us to compute the sizes of the three possible types of cavities existing in the face-centered cubic crystals. There are two types of interstitial holes, namely, tetrahedral holes, the centers of which are

equidistant from four noble gas atoms and octahedral holes in which they are equidistant from six. A substitutional hole is created when one atom is removed from a lattice site. The center of such a cavity is equidistant from twelve lattice sites and it is obviously the biggest hole. The radii of such cavities, together with other data concerning the noble gases, are given in Table I. The van der Waals radius of methane being $2.08 - 2.24 \text{ \AA}$, it seems obvious that the only type of hole which can possibly accommodate a methane molecule is at a substitutional site.

Crystal Imperfections or Surface Sites.

Microcrystals formed by spraying a gaseous mixture on a cold target are known to be highly imperfect. However, raising the temperature of the sample (annealing) allows the molecules or atoms to rearrange into a regular crystalline lattice. When the deposition is performed at higher temperatures (20° - 30°K) it seems that the molecules can rearrange at the surface of the solid being formed, thus giving a good crystal directly.

Spectra of samples deposited slowly at the lowest temperature ($\sim 5^{\circ}\text{K}$) always showed broad bands without much fine structure. Presumably these solids were not crystalline. On the other hand, almost every time the annealing operation was performed the fine structure appeared or improved. The narrowness of the lines observed ($1 \sim 2 \text{ cm}^{-1}$) indicates that the solute molecules are being subjected to highly reproducible matrix fields. This suggests that methane is not trapped at surface sites or crystal imperfections where the fields are unsymmetrical and not reproducible.

Low Symmetry of the Sites.

If we were to assume that some of the symmetry elements of the f.c.c.

crystal are lost in going from the pure crystal to the solid solutions, each active vibrational band of methane (symmetry F_2) would be split into two or three components. Since according to the foregoing analysis each methane molecule is isolated in the matrix, coupling cannot be invoked to account for the number of observed lines, at least four. Moreover this explanation could not account for the fact that a greater number of lines were found in the CD_4 than in the CH_4 spectra and it has to be rejected.

Free or hindered rotation.

If the solute molecules were rotating freely in the crystals one would expect rotational structure on the bands which would approximate that of the gas at the same temperature. In that case the lines ought to be equally spaced with a separation of 10 cm^{-1} for ν_3 and, as a consequence of Coriolis interaction between the internal angular momentum and the rotational angular momentum, of 4.7 cm^{-1} in the ν_4 (bending) band.

All of the spectra reported here show a smaller spacing for ν_3 in xenon; the spacings range from 5 to 8 cm^{-1} . Consequently one must discard the possibility of free rotation in favor of hindered rotation. On the other hand the line separation in the ν_4 region in xenon (CH_4) is about half that in the ν_3 region, showing clearly that rotational angular momentum is involved and that it is not far in magnitude from that of the free rotator. In this sense the spectrum of CH_4 in xenon appears to be that of a nearly free rotation.

However, there are further problems. The relative intensities of the various transitions of a free rotor at temperatures from 4.4°K to 15.0°K are shown in Tables III and IV. A six line pattern is expected in the

region from 0°K to 15°K , as a consequence of the fact that the three nuclear spin species, A, F and E occupy the levels $J = 0, 1$ and 2 at 0°K and the population ratio is 5:9:2 if there is no equilibration of the nuclear spin species. CH_4 in xenon shows only four lines and the examination of thicker films shows no trace of further lines. On the other hand the stretching region of CH_4 in krypton shows a fifth line (but near the center of the band) and all of the CD_4 spectra show many more peaks than expected for a free rotor. Consequently, although there is rotation in the sense that rotational angular momentum is present, the spectra can only be considered as those of a hindered rotor.

The assignment of each line to a specific transition is not so easily achieved in the case of a hindered rotor. Fortunately, King⁷ has developed the theory of the hindered rotational levels of a rigid tetrahedron in an octahedral field. He expanded the potential energy of the tetrahedron as a series in spherical rotor functions, so that successive terms can be designated by the corresponding quantum numbers. The first ($J = 0$) term is trivial since it gives only the constant term in the potential; the next two are $J = 4$ and $J = 6$ terms.

In the case of ionic crystals he showed that the $J = 4$ terms completely dominate so that the potential energy can be written in terms of a single parameter β , i.e.,

$$V(\theta, \psi, \chi) = \beta V_4(\theta, \psi, \chi)$$

where θ , ψ and χ are the Euler angles denoting the orientation of the tetrahedron and V_4 is the normalized $J = 4$ function. For NH_4^+ ions in a CsCl type lattice $\beta < 0$, while in a NaCl type lattice $\beta > 0$. In the CsCl lattice the nitrogen is at the center of a cube, the corners of which are occupied

by negative ions. For purely electrostatic interactions the NH_4^+ ion has its lowest potential energy when the N-H bonds are all directed along the cube diagonals toward the negative ions. In the NaCl case the negative ions are at the centers of the cube faces and this same orientation corresponds to a maximum potential energy.

The case of a methane molecule in a face centered cubic structure is related but different. If the carbon is at the center of a cube, the twelve closest rare gas atoms are at the mid-points of the cube edges. Furthermore, the interactions between the hydrogens and the rare gas atoms are probably repulsive, rather than attractive as in the NH_4^+ -negative ion case. Although we have not evaluated the resulting potential energy function it seems likely that in this case the potential energy minimum occurs when the hydrogens are oriented toward the cube corners, since in this orientation each proton is simultaneously at a maximum distance from three rare gas atoms. This would be the King negative β case. Of course, it may be necessary to include further terms such as V_6 in the potential function to get quantitatively correct levels, but the King calculations should yield a qualitatively correct picture of this situation with 24 minima.

Figures 8 and 9 show the behavior of the rotational energy levels of the rigid rotor subjected to an octahedral field, βV_4 . The absolute energy of the levels is given in Figure 8, while Figure 9 shows the same energy relative to the energy of the ground state. The potential energy function must be invariant both with respect to the octahedral rotations of the crystal field (O) and the tetrahedral rotations of the molecule (T). In addition, the presence of a center of symmetry in the octahedral field has the effect of making the potential energy invariant to cubic rotations about

the molecular axes. This can be visualized by realizing that if the tetrahedron is inscribed in a cube so that its apices coincide with four cube corners, the center of symmetry has the effect of generating another tetrahedron occupying the other four corners of the cube. Therefore, the energy levels can be classified as direct product representations of the direct product group $O \times \bar{O}$, where the first term refers to crystal axes and the second to molecular axes. The five levels $A_1 \times \bar{A}_1, F_1 \times \bar{F}_1, E \times \bar{E}, F_2 \times \bar{F}_2$ and $A_2 \times \bar{A}_2$, represent the complete set of hindered rotational levels which will give rise to the first librational state (24-fold degenerate) when the potential hindering rotation is large enough ($\beta < -50$). Another set of rotational levels (among them $F_2 \times \bar{E}, E \times \bar{F}_2, F_1 \times \bar{F}_1, F_2 \times \bar{A}_2, A_2 \times \bar{F}_2$ and others) collapses to give rise to the first excited librational state (72-fold degenerate). In ionic cases these excited librational levels lie some 300 cm^{-1} (NH_4I) to 500 cm^{-1} (NH_4F) above the ground state but in the present problem they would be expected at lower frequencies.

We are concerned chiefly with the region of small β . At the lowest temperatures only the levels originating ($\beta = 0$) in $J = 0, 1$ or 2 are populated to any extent and the A spin molecules are in the lowest $A_1 \times \bar{A}_1$ state, the F in the $F_1 \times \bar{F}_1$ state and those of E spin species in $E \times \bar{E}$. Since the allowed transitions are $A \leftrightarrow F, F \leftrightarrow E, F \leftrightarrow F$, the spectrum at low temperatures should show a Q branch which splits into $Q(1)$ and $Q(2)$ as β increases, $R(0)$ and $P(1)$ lines which converge only slowly as β increases, and an $R(1)$ line which converges rapidly toward $R(0)$ and splits into two components with increasing β . A weak $P(2)$ line is also expected, placed symmetrically with respect to $R(1)$. Since $J = 3$ is split into five components, all but one of which diverge from the ground state, $R(2)$ is expected to be weak and to be split into many components, all but one dis-

placed away from the band center. This behavior is illustrated in Fig. 10, where the solid lines indicate the transitions observable at the lowest temperature and the dotted lines indicate those which may appear as the temperature is raised.

Methane in Xenon (Figures 1a,b,c and d)

As mentioned before, CH_4 shows a similar four line pattern in the stretching (ν_3) and the bending (ν_4) regions which is very nearly that expected for free rotation if nuclear spins are equilibrated at the low temperature (Table III). The most intense line is presumably $\text{R}(0)(J=0 \rightarrow 1)$; on the low frequency side are $\text{Q}(1)(J=1 \rightarrow 1)$ and $\text{P}(1)(J=1 \rightarrow 0)$, while on the high frequency side is $\text{R}(1)(J=1 \rightarrow 2)$. This much is straightforward but the absence of $\text{P}(2)(J=2 \rightarrow 1)$ particularly needs explanation. The absence of $\text{R}(2)$ can be accounted for by the high degree of splitting of the $J=3$ level.

If spins are equilibrated at 5°K the absence of these lines, both of which originate in the $J=2$, $\text{E} \times \bar{\text{E}}$ level follows naturally, as does the very great intensity of $\text{R}(0)$. Nevertheless, the intensity ratios do not change as the temperature is raised to 16°K (Fig. 1c) so that there can be no conversion of A to F species molecules as required to maintain the equilibrium; otherwise $\text{R}(0)$ should have dropped in intensity relative to $\text{R}(1)$, $\text{P}(1)$ and $\text{Q}(1)$. This observation seems to oppose the idea of equilibrated spins unless the equilibration takes place during condensation. An alternative possibility is that if $\beta = -4$ the $\text{E} \times \bar{\text{E}}$ component of $\text{R}(1)$ would be hidden under $\text{R}(0)$. In that case, since all of the molecules of E spin species are in the $\text{E} \times \bar{\text{E}}$ level at 5°K ., the $\text{P}(2)$ line would coincide with $\text{P}(1)$, even for a room temperature spin distribution. This latter suggestion is

consistent with what is found in the krypton crystal.

The decrease in spacing in ν_3 (no Coriolis coupling) from 10 cm^{-1} ($R(0)$ and $Q(1)$, $Q(1)$ and $P(1)$) is accounted for satisfactorily if $\beta = -4$ to -5 in King's model. Since in King's model the barrier to rotation about a 4-fold crystal axis is $-2.5b\beta$, this corresponds to a barrier of $50 - 60\text{ cm}^{-1}$. To test the reasonableness of this last conclusion this barrier was independently calculated. The interactions were expressed either by a Lennard-Jones (12-6) or a modified Corner-Buckingham (Exp-6) potential¹¹ with parameters mixed in the usual way with those of a modified

11. J.O. Hirschfelder, C.F. Curtiss and R.B. Bird, *Molecular Theory of Gases and Liquids* (John Wiley and Sons, Inc., New York 1954).

deBoer potential^{12,13}. In the derivation of the barriers from a Lennard-

12. J. deBoer, *Physica*, 9, 363 (1942).

13. K.S. Pitzer and E. Catalano, *J. Am. Chem. Soc.*, 78, 4844 (1956).

Jones potential it was assumed that the interactions between a methane molecule and the rare gas atoms were well approximated by the interactions, with the lattice, of four helium atoms situated at the positions occupied by the four hydrogen atoms of the methane molecule. In both approaches the heights of the barriers were found to be of the order of 10-50 calories per mole in xenon and krypton but 500 calories per mole in solid argon.

The position of $R(1)$ (Fig. 10), as has been pointed out, is consistent with $\beta = -4$ only if one of its components coincides with $R(0)$. This would also explain the absence of $P(2)$. Nevertheless, the great intensity of $R(0)$ seems to demand spin equilibration at a temperature near 5°K .

In summary, the spectrum of CH_4 in xenon can be reasonably well accounted for only if (a) nuclear spins are equilibrated between 5.5°K and

8.0°K and the ratio of spin species does not change in warming the 16°K (b) the King β is -5 to -5, corresponding to a barrier of about 50-60 cm^{-1} about the 4-fold crystal axis and (c) the Coriolis interaction in ν_4 is nearly that in a free molecule, implying that the rotation is only very slightly hindered, even in these low J states.

CH₄ in Krypton (Figs. 2a, b and c).

Except for a shift of about 1.4 cm^{-1} to higher frequencies, the bending region is substantially the same as in xenon. However, the effect of the smaller cavity shows up in the stretching region in two ways. The entire spectrum is shifted about 11.4 cm^{-1} to higher frequencies, as might be anticipated as a result of the repulsive interaction with the rare gas cage. In addition, although the spacing between R(0)(3024.8 cm^{-1}), Q(1)(3016.6 cm^{-1} and P(1)(3008.3 cm^{-1}) is nearly the same as in xenon, the R(1) line at 3028.4 cm^{-1} is moved in closer and a new line appears at 3022.2 cm^{-1} . This is closely in accord with King's analysis which predicts a splitting of the J=2 level. In that case the line at 3022.2 cm^{-1} corresponds to the transition from J=1 to the $\text{Ex}\bar{\text{E}}$ level and that at 3028.4 cm^{-1} to the transition to the $\text{F}_2 \times \bar{\text{F}}_2$ level. According to Fig. 10 this would occur at about $\beta = -5$. It also suggests that in xenon the same splitting may occur but that one of the components ($\text{Ex}\bar{\text{E}}$) of J=2 is superimposed on R(0) as would occur at $\beta = -4$.

CH₄ in Argon (Figures 3a, b, c, d).

Whereas in xenon and krypton the CH₄ spectrum showed no tendency to change in time or to change upon annealing at higher temperatures, the argon spectrum clearly shows the effect of diffusion to form CH₄ aggregates. Fig. 3a shows the spectrum of a freshly deposited film. After annealing

at 30-35°K for a few minutes and cooling again, the band at about 3013 cm^{-1} develops. After a second heating to 30-35°K this band develops further. It is not clear whether the fine structure which develops at 3038.2 cm^{-1} and 3029.8 cm^{-1} is also due to the aggregates or whether it is simply better resolved after the crystal is annealed. In any case it is clear that the peaks at 3021.4, 3028.2, 3033.0, 3037.0 and 3041.8 cm^{-1} are due to isolated molecules while the three low frequency lines arise from pairs of higher multiplets. The five singlet lines form a spectrum not unlike that in krypton, with perhaps a slightly higher value of β . In that case R(1) is the doublet at 3041.8 cm^{-1} and 3033.0; R(0) is at 3037 cm^{-1} ; Q(1) is at 3028.2 cm^{-1} and P(1) at 3021.4 cm^{-1} .

This is a rather surprising conclusion in view of the much greater compression of the CH_4 molecule if the cavity actually has the dimensions of a substitutional cavity in the undistorted argon crystal. It must therefore be supposed that the argon crystal is locally distorted so that the cavity is enlarged, the resultant strain being distributed through several layers of argon rather than concentrated on the CH_4 molecules. Some increase in the compression is also clear from the further shift of the stretching region to high frequencies, some 27 cm^{-1} above that in xenon.

It is not possible to say much in detail about the bending region since the spectrum, Fig. 3d, was taken on the same specimen as Fig. 3c and contains CH_4 aggregates as well as isolated CH_4 molecules. Nevertheless, with the exception of a small shoulder on the main peak it, like the krypton case, has four peaks, the mean being shifted about 7 cm^{-1} to higher frequencies. The spacing between peaks is again much smaller than in the stretching region, showing the presence of a strong Coriolis coupling,

so that as in the other gases the rotation is only slightly hindered.

CD₄ in Xenon and Krypton Crystals.

The CD₄ spectra all show much more fine structure than CH₄ and we have not been able to interpret them in detail. However, it is possible to reach some conclusions from Figs. 8 to 10. From the form of the Schrödinger equation,

$$\nabla^2\psi + \frac{8\pi^2}{h^2} (mE - m\beta V_4)\psi = 0$$

the calculations for CH₄ can be applied to CD₄ except that the effective value of β (for the same physical potential) is twice as great and the calculated energies are twice the correct ones. Therefore we expect to find the CD₄ levels in the vicinity of $\beta = -8$. The effect of the mass on the energy scale is already taken care of by the different value of B appropriate to CD₄. We therefore expect a much more highly perturbed spectrum with a width between extreme peaks of about 9 cm⁻¹. This is in fact what is observed.

CD₄ in Xenon (Figs. 5a, b, c and d).

The spectrum in the stretching region is not very different from that of CH₄. Comparison with Table IV suggests that spins are equilibrated at a temperature a little above 5°K and that the Q branch is the peak at 2248 cm⁻¹. In that case 2250.6 cm⁻¹ is R(0) and R(1) is split into a component at 2253.4 cm⁻¹ and one buried in R(0). There is no reason why P(1) should be split so the extra peak at 2244.3 cm⁻¹ may be a component of P(2).

The choice of 2247.0 cm⁻¹ as the Q branch is confirmed by the fact that it becomes the most intense peak at 16°K and 30°K. Similarly,

990.2 cm^{-1} must be the Q branch of the bending band. Then $R(0) = 991.2 \text{ cm}^{-1}$, $R(1) = 993.5 \text{ cm}^{-1}$, $P(1) = 988.7 \text{ cm}^{-1}$, $P(2) = 987.1 \text{ cm}^{-1}$ (ExE), 985.9 cm^{-1} ($F_2 \times F_2$) and $P(3) = 982.9 \text{ cm}^{-1}$ becomes the most reasonable assignment. In the absence of a theoretical calculation including V_6 and Coriolis interactions, it does not seem possible to test this assignment more exactly.

CD₄ in Krypton (Figs. 6a and b).

The spectrum bears a close resemblance to that in xenon but there is still further splitting. There seems little doubt that $R(1) = 2262.1 \text{ cm}^{-1}$, $R(0) = 2260.3 \text{ cm}^{-1}$, and that 2257.2 cm^{-1} is one of the components of the Q branch. However, it is not clear whether 2258.4 cm^{-1} is a component of $R(1)$ or the Q branch. The lower frequency lines are presumably $P(1)$ and $P(2)$. Similar considerations apply to the bending spectrum.

If in both krypton and xenon $R(1)$ is well resolved from $R(0)$ one cannot escape the conclusion that $2B$ is substantially less than 10 , perhaps as small as 5 or 6 . The entire spectrum fits better in this case, which leads to a barrier estimate substantially smaller than in CH_4 or perhaps $30 - 40 \text{ cm}^{-1}$. It appears, though, that the barrier is high enough to reduce the angular momentum substantially since comparison of ν_3 and ν_4 in CD_4 shows much less Coriolis interaction than in CH_4 . This would be expected as the levels dropped beneath the barrier tops.

Frequency Shifts

The matrix shift, $\Delta\nu$, may be defined as the shift in the position of the Q branch that occurs in going from the gas to the solid solutions spectra. Table V indicates the magnitude of the observed shifts for the two infrared active bands, ν_3 and ν_4 , of CH_4 and CD_4 (Fig. 3a). The gas-

phase frequencies, ν_3 and ν_4 , obtained under similar conditions were found to be at 3018.4 and 1306.2 cm^{-1} respectively for CH_4 and 2259.0 and 995.5 cm^{-1} for CD_4 .

The shift toward the blue can be thought of as arising from short-range repulsive forces between the solute molecules and the noble gas atoms. The smaller the hole occupied in the matrix, the larger the observed blue shift. On the other hand, the large red shifts found in xenon solutions are not well understood.

The shifts of CH_4 were computed using the K.B.M. relation¹⁴ in the

 14. E. Bauer and M. Magat, J. Phys. Radium, 9, 319 (1938).

form given by Bell and McKean¹⁵. The values of the intensity of absorp-

 15. D.F. Bell and D.C. McKean Spectrochim. Acta, 18, 1029 (1962).

tion of CH_4 and CD_4 necessary for these calculations were taken from their paper. The shifts computed in this way are much smaller (Table VII) than the observed red shifts in solid xenon. However, it seemed worthwhile pointing out an obvious failure of the K.B.M. relation for a case where all the parameters are well defined.

Ratio of the Intensities of the Absorption Bands, ν_3/ν_4 .

Nothing can be said about the absolute intensities of absorption of the ν_3 or ν_4 vibrations in the present study, since the sample thicknesses are unknown. However, the ratio of the intensities of the two bands, ν_3 and ν_4 , obtained with the same sample should be meaningful. It can be compared with the ratio of the band intensities measured in the gas phase at room temperature. Data reported in the literature are collected in

Table VI. For CH_4 and CD_4 gases the mean intensity ratios of ν_3 and ν_4 are 2.16 and 1.55 respectively, whereas the average ratios observed in the present study are both around 1.0 for CH_4 and CD_4 . This discrepancy points to a significant difference in the influence of the matrices on the stretching and bending modes of CH_4 and CD_4 .

CONCLUSION

It seems reasonably clear, altogether, that the fine structure in the vibration bands of both CH_4 and CD_4 as substitutional impurities in rare gas crystals can be ascribed to the quantized levels of a slightly hindered rotor with barriers of the order of 50 cm^{-1} high.

The theory of King, based on a rigid tetrahedron moving in a field βV_4 , gives a satisfactory semi-quantitative account of the observations but it is still in need of further refinement. A study of the effect of V_6 terms in the potential is in progress and it may be hoped that their inclusion will improve this situation.

As regards the rotation of other molecules in rare gas crystals, it seems likely that the barriers to rotation, and the perturbations of the rotational spectra, will be at least as great and probably greater than for the highly symmetrical molecules CH_4 and CD_4 .

ACKNOWLEDGMENT

We should like to acknowledge many stimulating discussions with Dr. S. Kimel which contributed a great deal to the progress of this work.

TABLE I - Data on Rare Gas Crystals

| | C.C.d. ^a | S. | O. | T. | V.der W. |
|---------|---------------------|------|------|------|----------|
| Argon | 5.31 ± 0.01 | 1.85 | 0.74 | 0.39 | 1.91 |
| Krypton | 5.68 ± 0.03 | 2.00 | 0.82 | 0.45 | 2.01 |
| Xenon | 6.1 ± 0.1 | 2.20 | 0.85 | 0.54 | 2.20 |

Note: All the dimensions are expressed in Angstroms.

C.C.d. cubic cell dimensions

S radii of substitutional holes

O radii of octahedral holes

T radii of tetrahedral holes

V.der W. Vander Waals radii of the atoms. (Taken from Wyckoff Tables)

a Taken from: E. R. Dobbs and G. O. Jones, Reports on Progress in Physics (The Physical Society of London 1957) Vol. XX p. 560

TABLE II - vander Waals Radii

| | | | |
|------------------|---------|-----|---------|
| H ₂ O | 2.15 Å° | HCl | 2.48 Å° |
| NH ₃ | 2.19 Å° | HBr | 2.63 Å° |
| CO | 2.20 Å° | HI | 2.82 Å° |
| CH ₄ | 2.24 Å° | | |

This table was derived using the data from:

L. Pauling, The Nature of the Chemical Bond. 3rd edition Cornell (1960) p. 260 and 224.

TABLE III - Intensities of the rotation-vibration transitions of Methane.

| | No spin equilibration | | | spin equilibration | |
|------------------|-----------------------|-------|--------|--------------------|-------|
| | 4.4°K | 8.8°K | 13.2°K | 4.4°K | 8.8°K |
| R ₍₂₎ | 6 | 7 | 10 | - | 3 |
| R ₍₁₎ | 31 | 30 | 26 | 13 | 33 |
| R ₍₀₎ | 31 | 31 | 31 | 77 | 36 |
| Q | 23 | 23 | 23 | 8 | 21 |
| P ₍₁₎ | 6 | 6 | 5 | 2 | 7 |
| P ₍₂₎ | 3 | 3 | 4 | - | - |

TABLE IV - Intensities of the rotation-vibration transitions of Deuteromethane.

| | No spin equilibration | | | Spin equilibration | |
|------------------|-----------------------|--------|--------|--------------------|------|
| | 5.0°K | 10.0°K | 15.0°K | 5°K | 10°K |
| R ₍₄₎ | - | - | 1.5 | - | - |
| R ₍₃₎ | - | 3 | 7 | - | 3 |
| R ₍₂₎ | 9 | 15 | 16 | 4 | 14 |
| R ₍₁₎ | 34 | 25 | 18 | 34 | 28 |
| R ₍₀₎ | 19 | 16 | 13 | 30 | 12 |
| Q | 27 | 28 | 29 | 23 | 25 |
| P ₍₁₎ | 7 | 5 | 3.6 | 7 | 6 |
| P ₍₂₎ | 4 | 6 | 6.8 | 2 | 6 |
| P ₍₃₎ | - | 2 | 4.0 | - | 2 |
| P ₍₄₎ | - | - | 1.0 | - | - |

TABLE V. Frequency Shifts

| | CH ₄ | | CH ₄ | | CD ₄ | |
|---------|------------------------------------|---------------|------------------------------------|---------------|------------------------------------|---------------|
| | Observed Shifts(cm ⁻¹) | | Computed Shifts(cm ⁻¹) | | Observed Shifts(cm ⁻¹) | |
| | $\Delta\nu_3$ | $\Delta\nu_4$ | $\Delta\nu_3$ | $\Delta\nu_4$ | $\Delta\nu_3$ | $\Delta\nu_4$ |
| Argon | +14.9 | +1.2 | -0.6 | -0.7 | - | - |
| Krypton | - 1.8 | -3.9 | -0.6 | -0.7 | -1.2 | -3.3 |
| Xenon | -12.7 | -6.6 | -0.9 | -1.0 | -10.9 | -5.3 |

A positive number refers to a blue shift and a negative number to a red shift.

TABLE VI. Experimental intensities of the bands ν_3 and ν_4 of CH₄ and CH₄.
(Units: cm⁻²atm⁻¹)

| | ν_3 | 323 ^a | 270 ^b | 322 ^c | 342 ^e | 326 ^f | 306 ^h | 116 ^h | 153 ^g |
|-----------------|---------------|------------------|------------------|------------------|------------------|------------------|------------------|------------------|------------------|
| CH ₄ | ν_4 | 148 ^a | 135 ^b | 142 ^d | 164 ^e | 155 ^g | 130 ^h | 96 ^h | 87 ^g |
| | ν_3/ν_4 | 2.18 | 2.00 | 2.26 | 2.08 | 2.10 | 2.35 | 1.21 | 1.76 |

- | | |
|------------------------------------|---|
| a) R. Rollefson and R. Havens | Phys.Rev. <u>57</u> , 710(1940)(from refraction spectrum) |
| b) A. M. Thorndike | J.Chem.Phys. <u>15</u> , 868(1947). |
| c) H. L. Welsh et al | J.Chem.Phys. <u>19</u> , 340(1951). |
| d) H. L. Welsh et al | J.Chem.Phys. <u>20</u> , 1646(1952) |
| e) R. M. Armstrong and H. L. Welsh | Spectro Chim.Acta <u>16</u> , 840(1960). |
| f) J. Heicklen | Spectro Chim.Acta <u>17</u> , 201 (1961) |
| g) E. Ruf | Thesis, Univer. of Minnesota (quoted in f) |
| h) R. E. Hiller and J. W. Straley | J.Mol.Spectroscopy <u>5</u> , 24(1960) (indirectly) |

FIGURES

Note: All the spectra were obtained from annealed samples unless otherwise noted. On the left hand side the stretching region is reported while the bending is on the right hand side. The scale on the abscissa is cm^{-1} whereas the ordinate is $\log I/I_0$.

Figure 1a - 1% CH_4 in xenon at 5°K.

Figure 1b - 1% CH_4 in xenon at 16°K.

Figure 1c - 2% CH_4 in xenon at 5°K; the thickness of the sample is not the same in both regions.

Figure 1d - 5% CH_4 in xenon at 5°K.

Figure 2a - 0.75% CH_4 in krypton at 5°K.

Figure 2b - 0.75% CH_4 in krypton at 16°K.

Figure 2c - 0.75% CH_4 in krypton at 30 K.

Figure 3a - 0.2% CH_4 in argon at 16°K. This spectrum was recorded immediately after deposition at 16°K, without annealing the sample.

Figure 3b - Same sample as in figure 3a after the temperature was raised to 30-35°K for a few minutes and lowered again to 5°K.

Figure 3c - Same as 3b after the same operation was repeated.

Figure 3d - Bending vibration of the sample whose stretching vibration was reported in 3c.

Figure 4 - Stretching and bending frequencies of CH_4 in noble gas crystals.

Figure 5a - 0.5% CD_4 in xenon at 5°K.

Figure 5b - 2.0% CD_4 in xenon at 5°K.

Figure 5c - 2.0% CD_4 in xenon at 16°K.

Figure 5d - Stretching region of 2.0% CD_4 in xenon at 30°K.

Figure 6a - 0.5% CD_4 in krypton at 5°K.

Figure 6b - 0.5% CD_4 in krypton at 20°K.

Figure 7 - Stretching and bending frequencies of CD_4 in krypton and xenon crystals.

Figure 8 - Energy levels of King's hindered rotor.

$$1 = A_1 \times \overline{A_1} \text{ from } J = 0$$

$$2 = F_1 \times \overline{F_1} \text{ from } J = 1$$

$$3 = F_2 \times \overline{E} \text{ from } J = 2$$

$$E \times \overline{F_2}$$

$$4 = F_2 \times \overline{F_2} \text{ from } J = 2$$

$$5 = E \times \overline{E} \text{ from } J = 2$$

$$6 = F_1 \times \overline{A_2} \text{ from } J = 3$$

$$A_2 \times \overline{F_1}$$

$$7 = F_2 \times \overline{F_1} \text{ from } J = 3$$

$$F_1 \times \overline{F_2}$$

$$8 = F_1 \times \overline{F_1} \text{ from } J = 3$$

$$9 = F_2 \times \overline{A_2} \text{ from } J = 3$$

$$A_2 \times \overline{F_2}$$

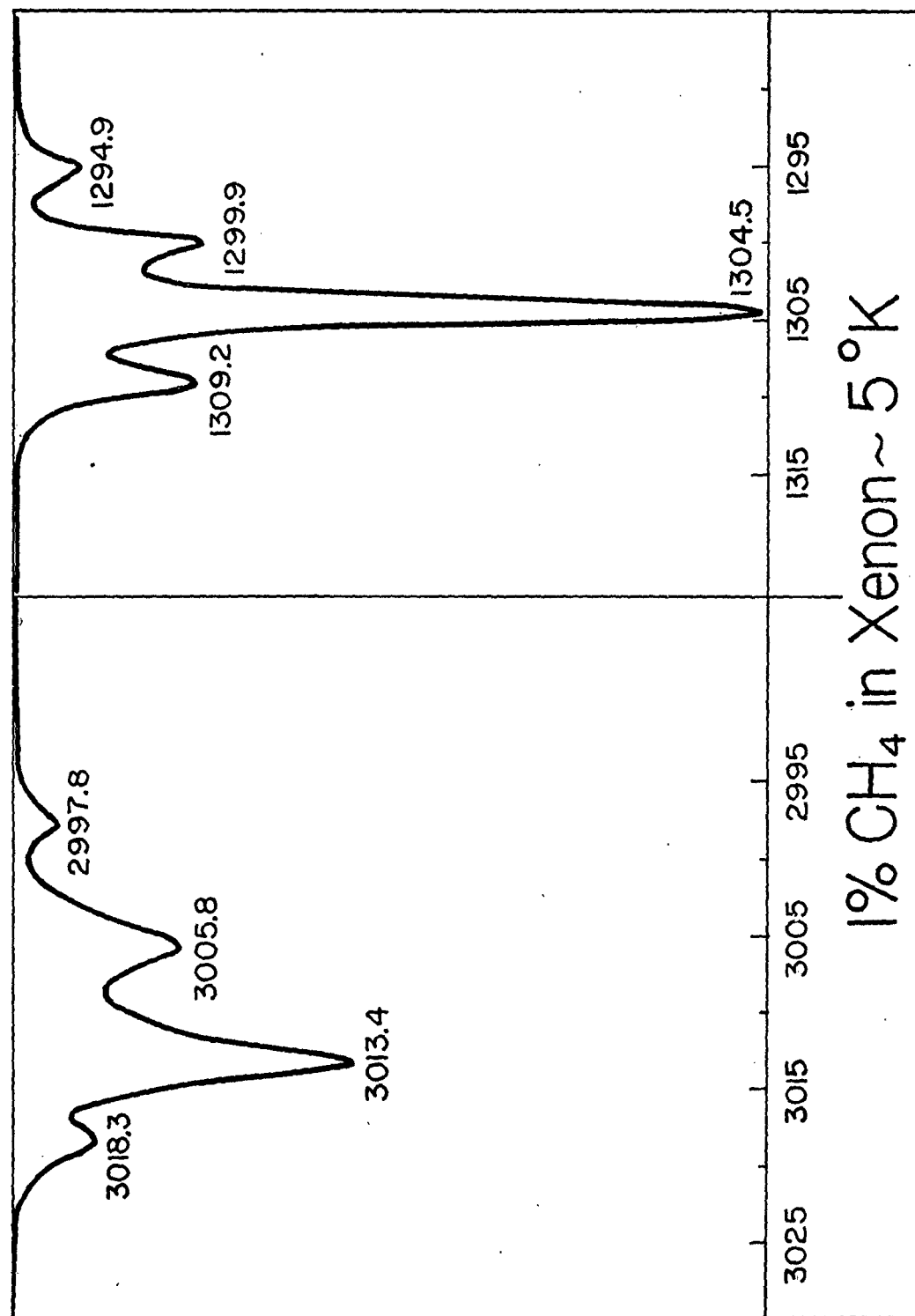
$$10 = A_2 \times \overline{A_2} \text{ from } J = 3$$

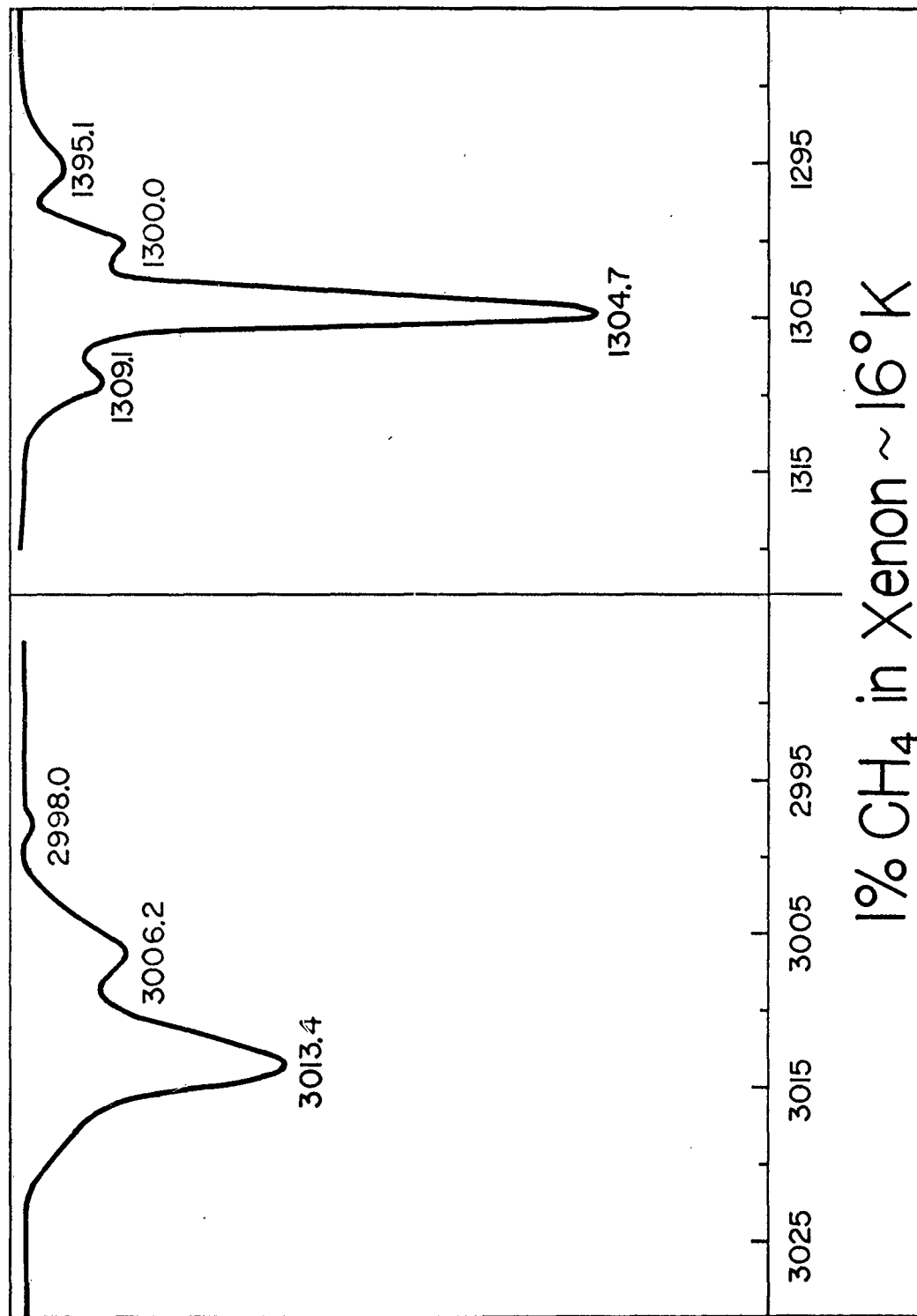
$$11 = F_2 \times \overline{A_1} \text{ from } J = 4$$

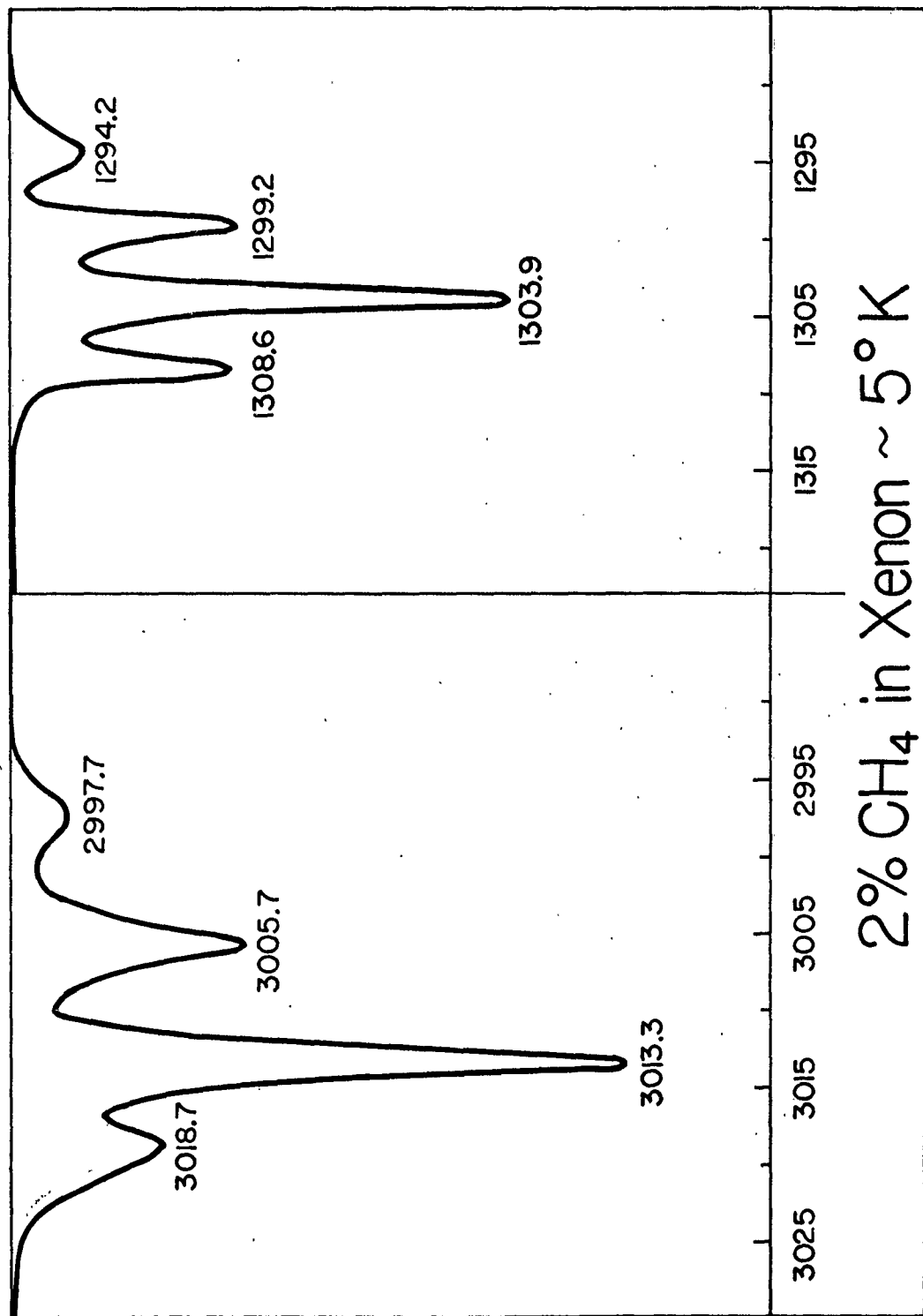
$$A_1 \times \overline{F_2}$$

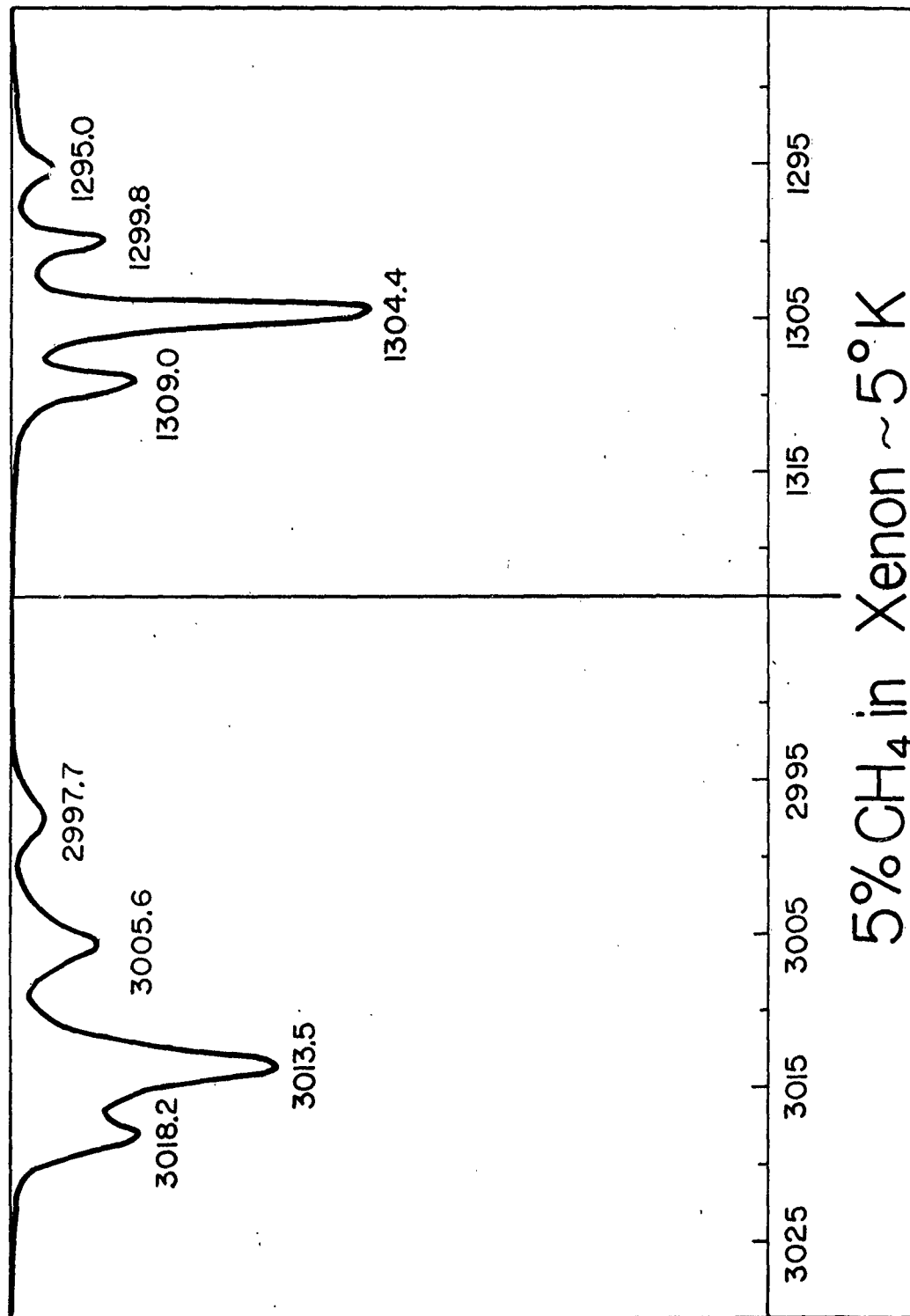
Figure 9 - Energy levels of King's hindered rotor relative to the ground state.

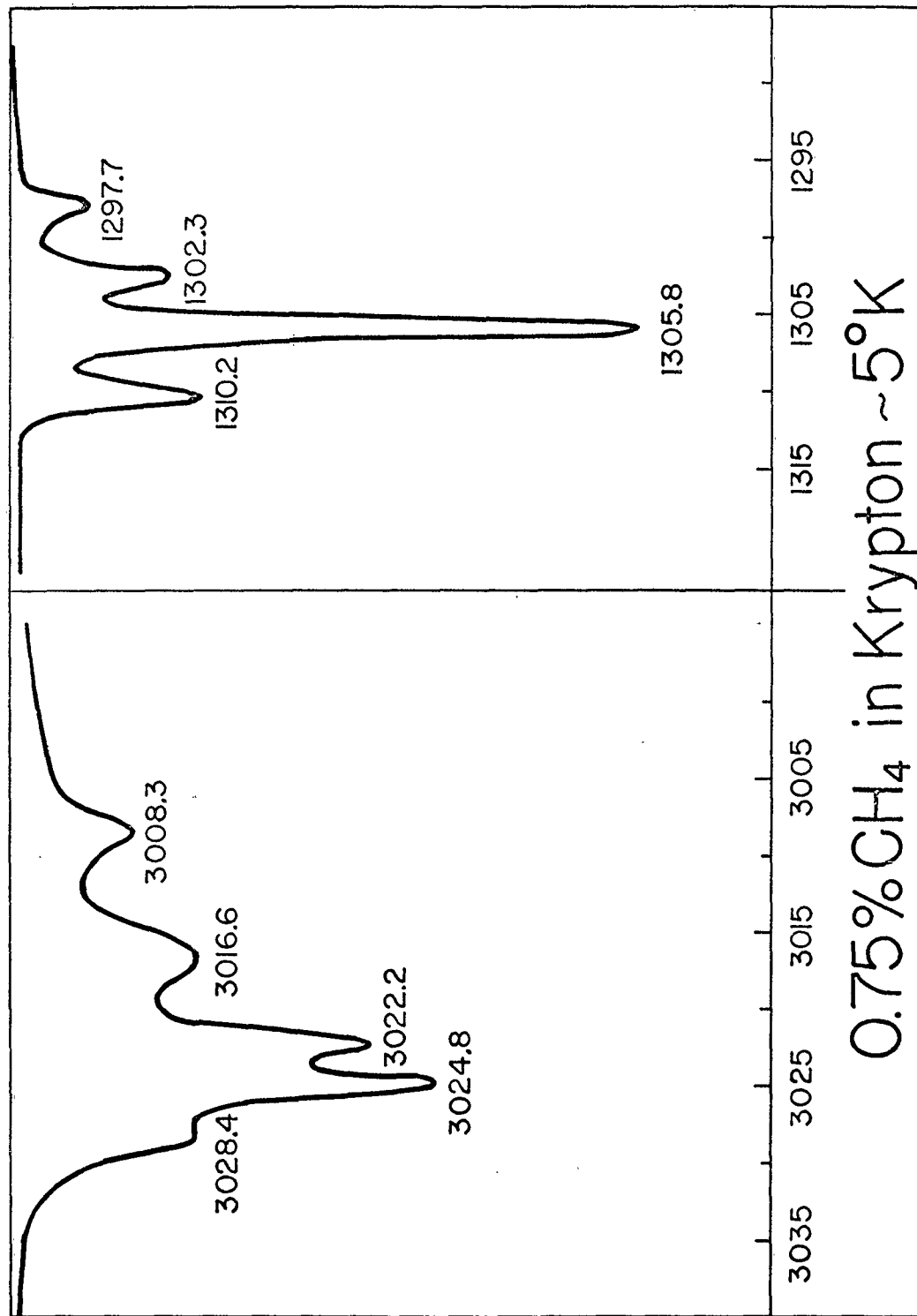
Figure 10 - Rotation-vibration transitions of King's hindered rotor. The full lines indicate the transitions that would occur at 0°K if the spins are not equilibrated.

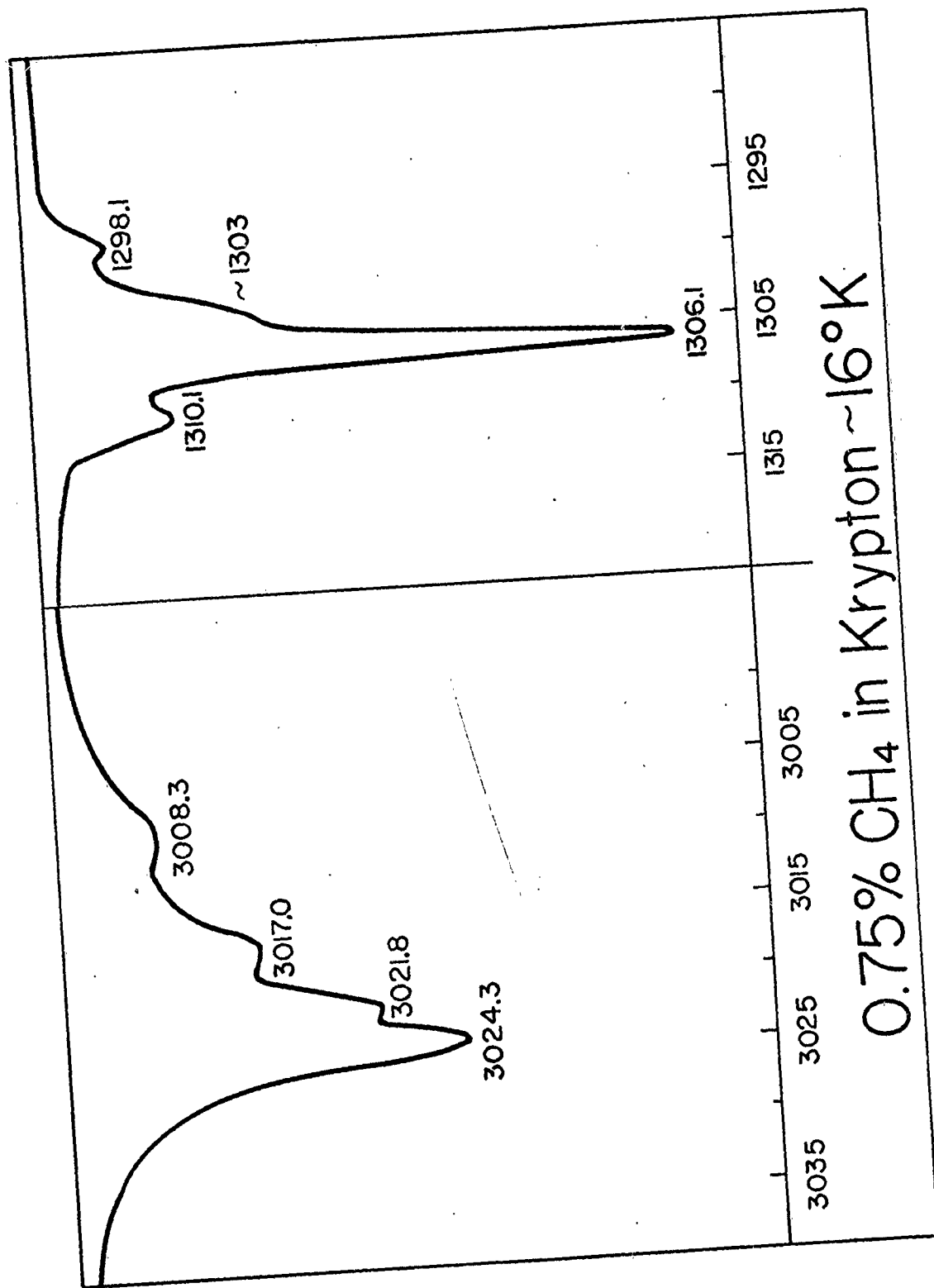


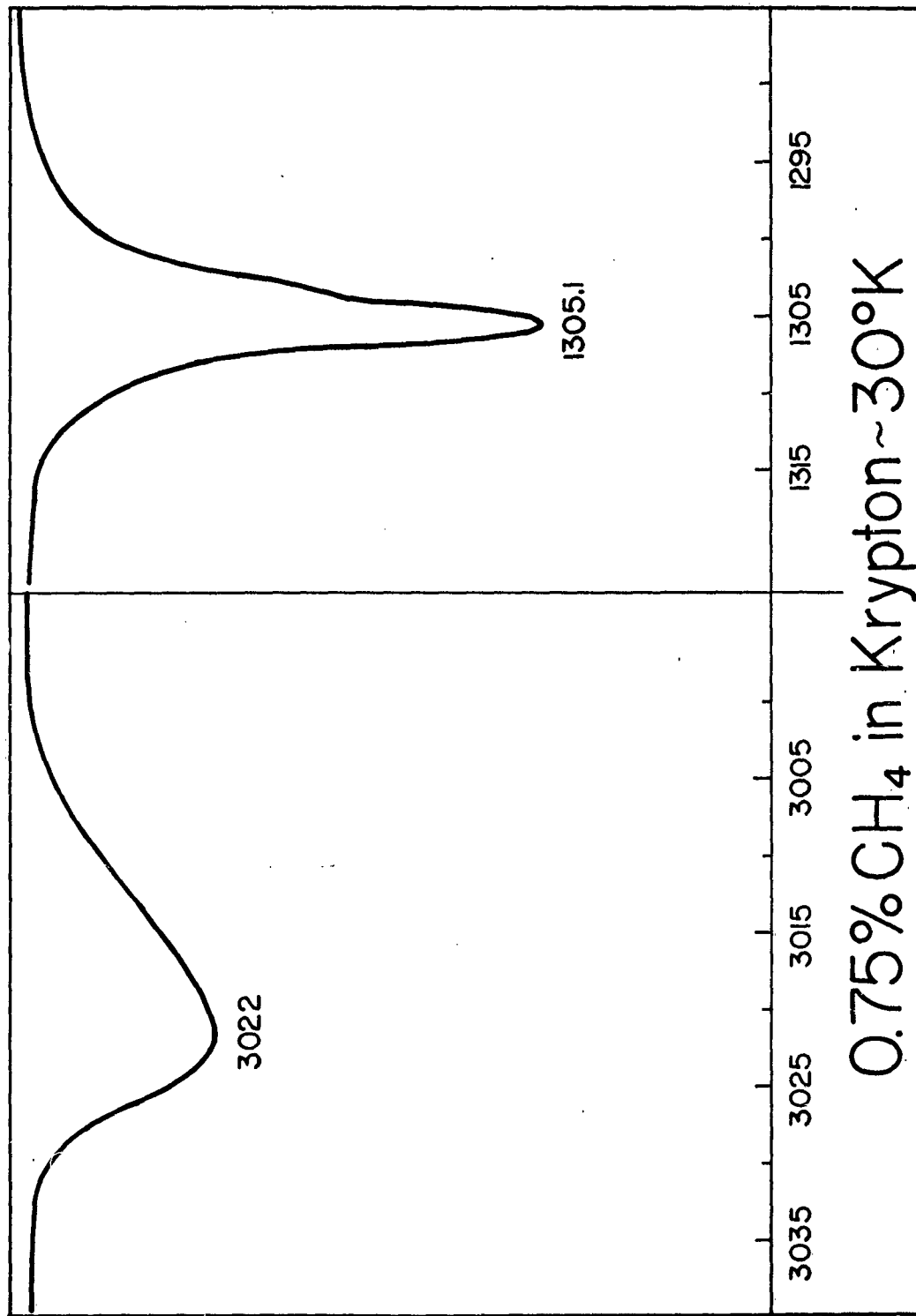


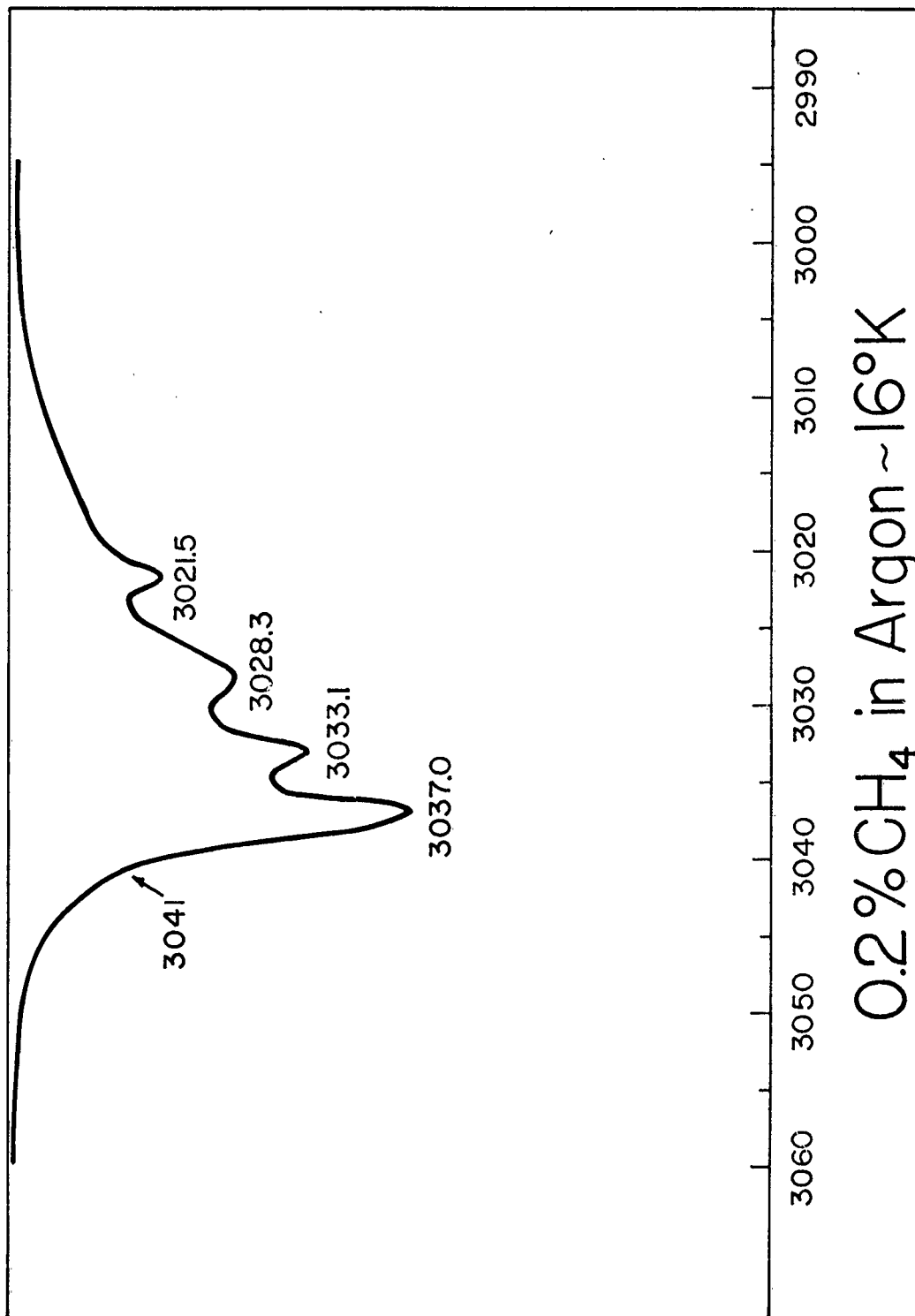


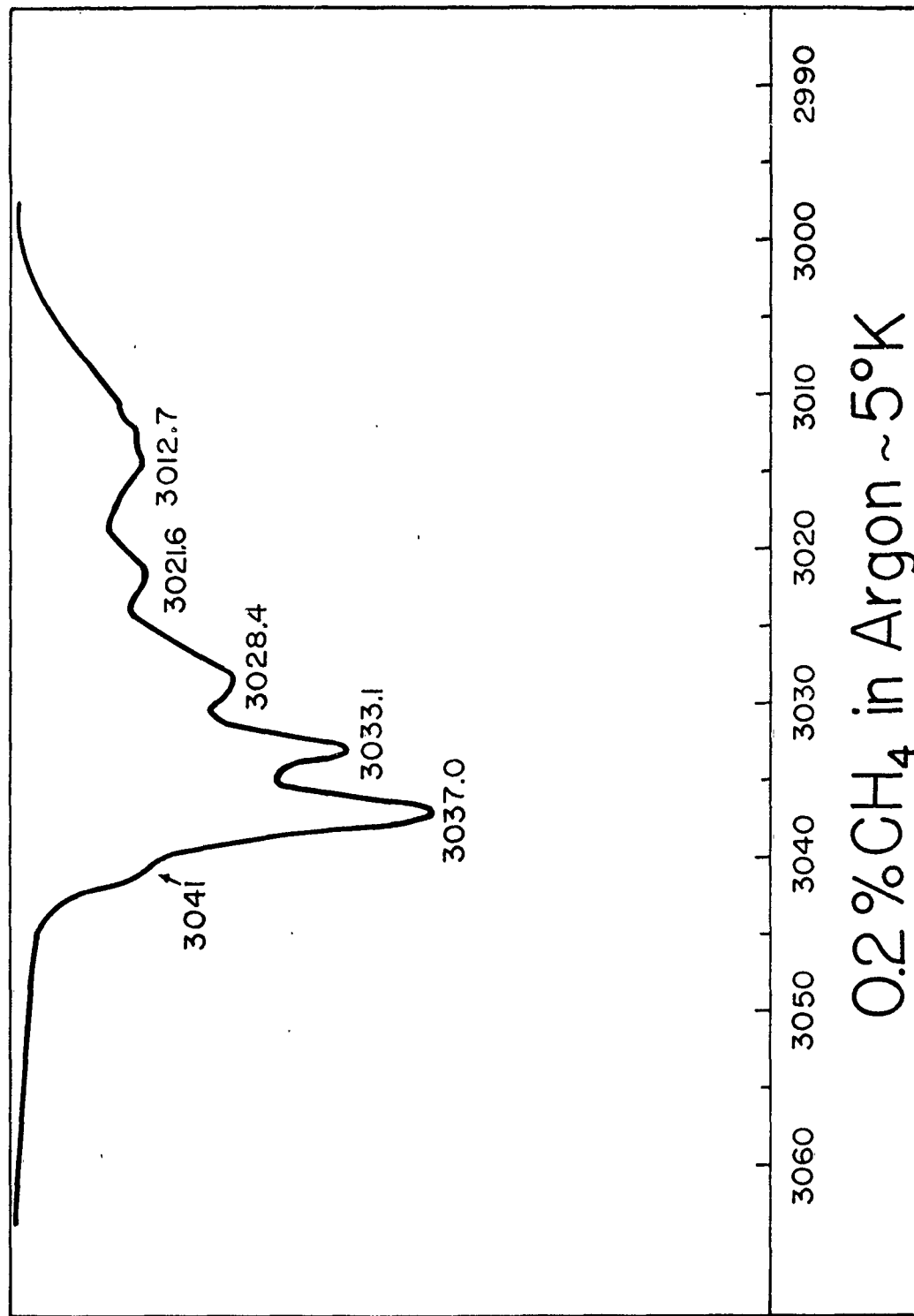


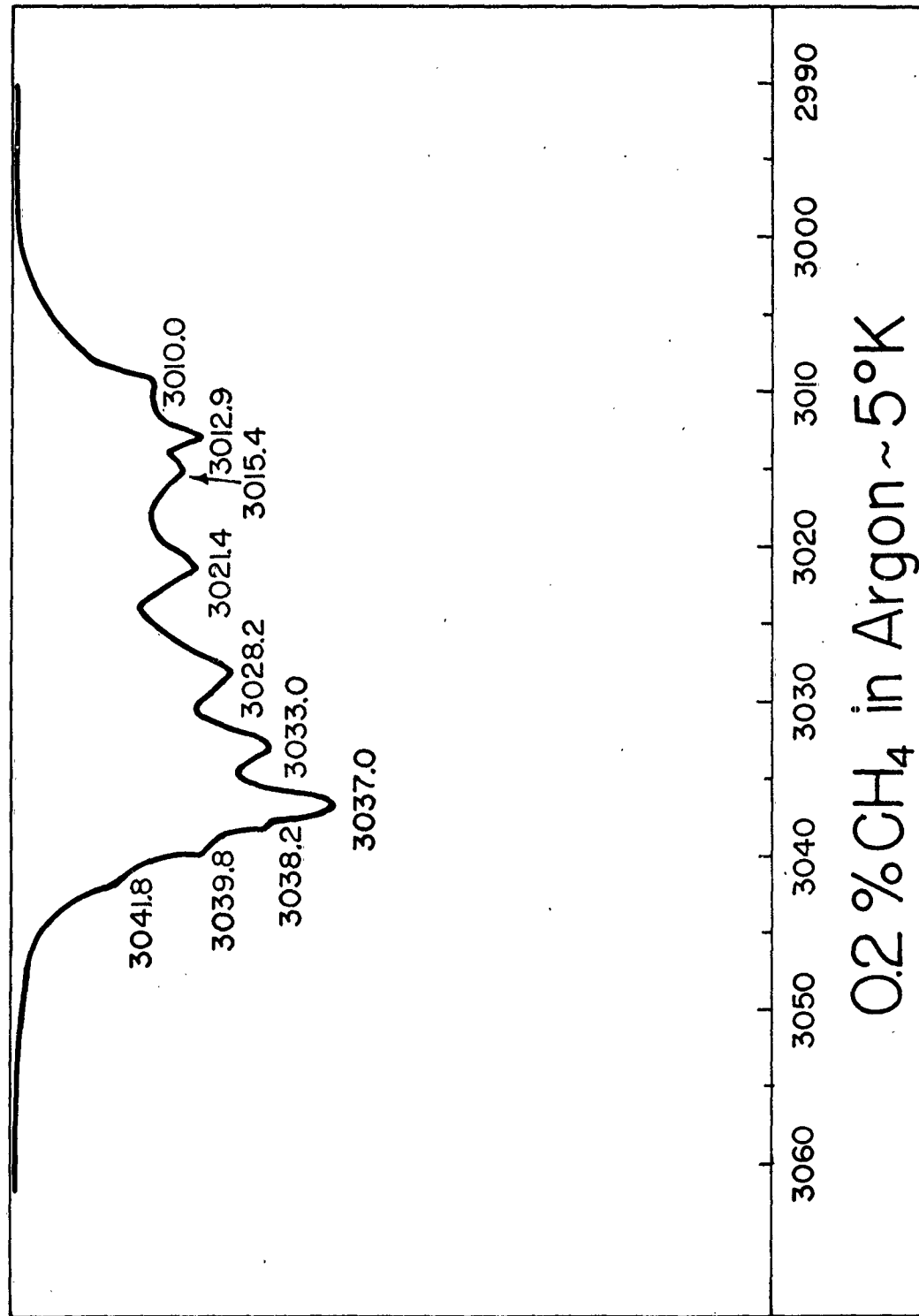


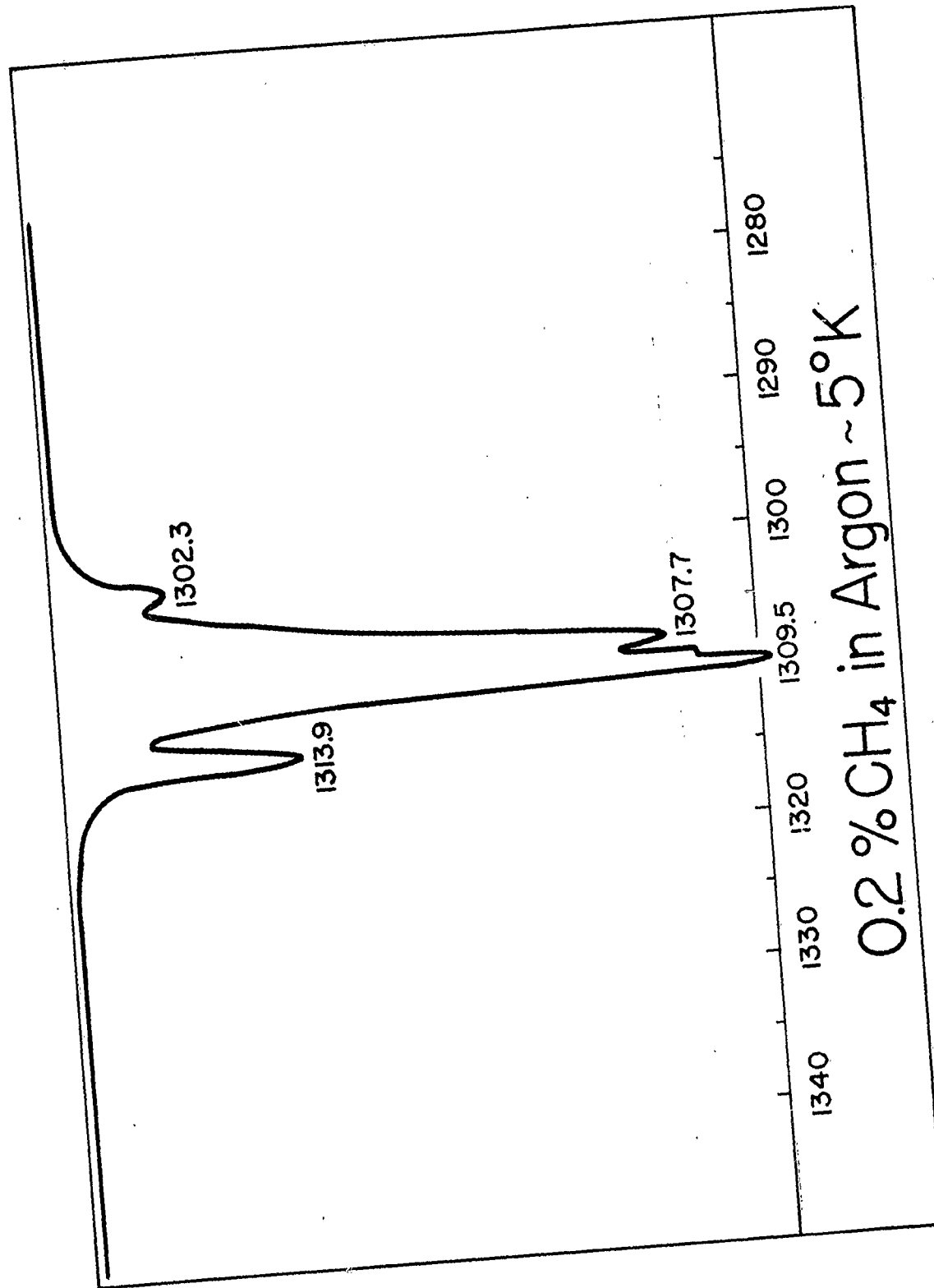


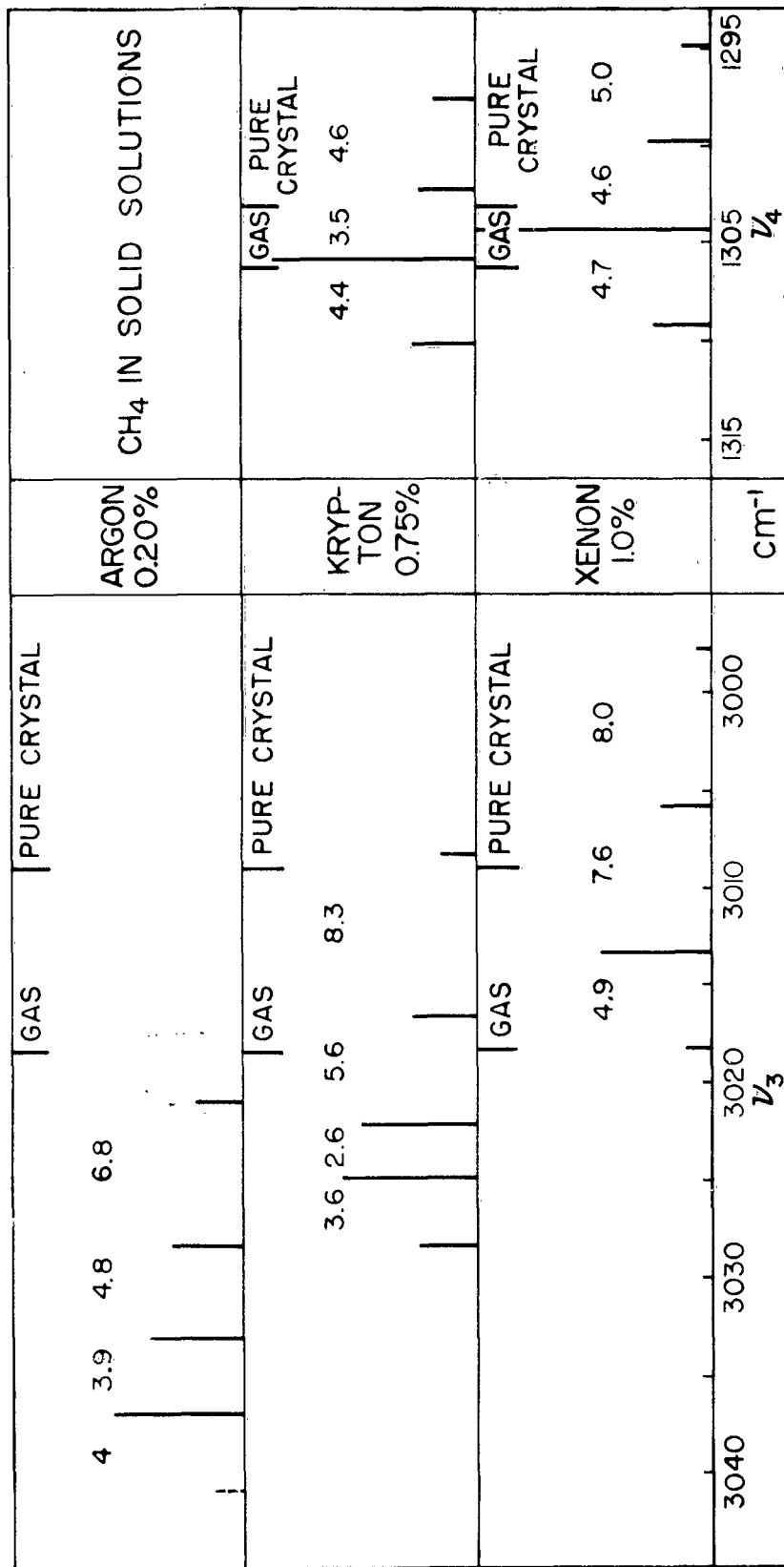


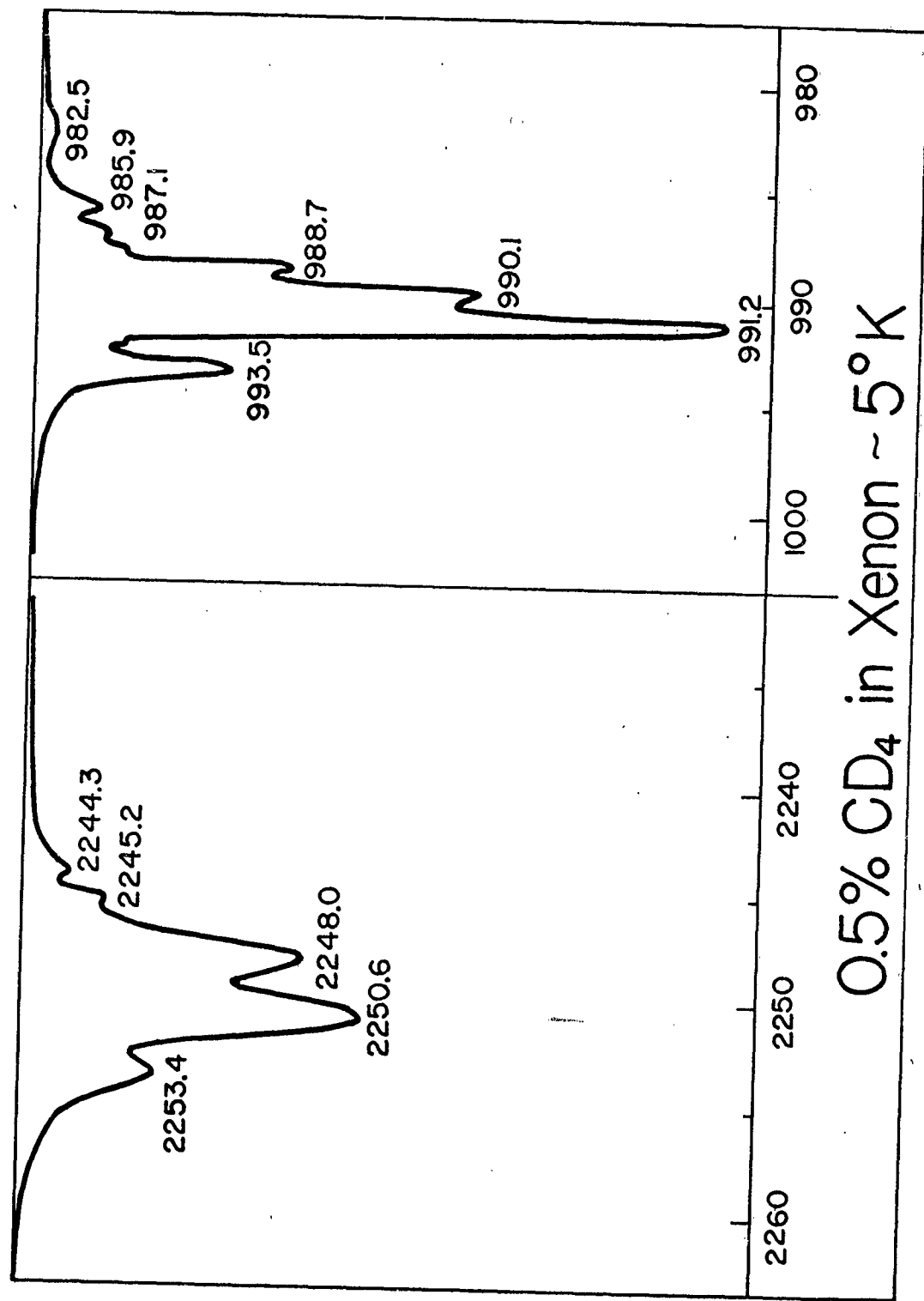


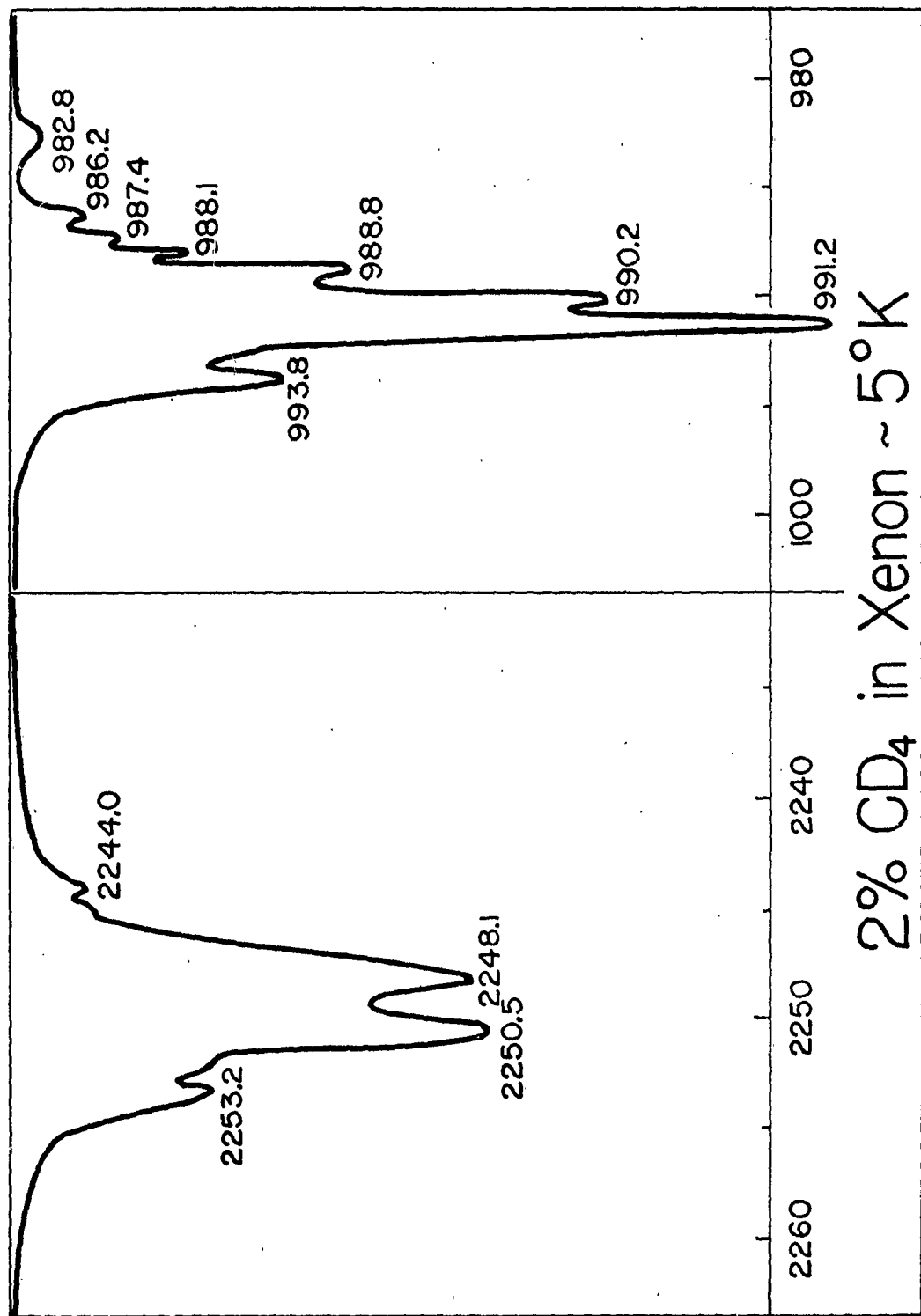


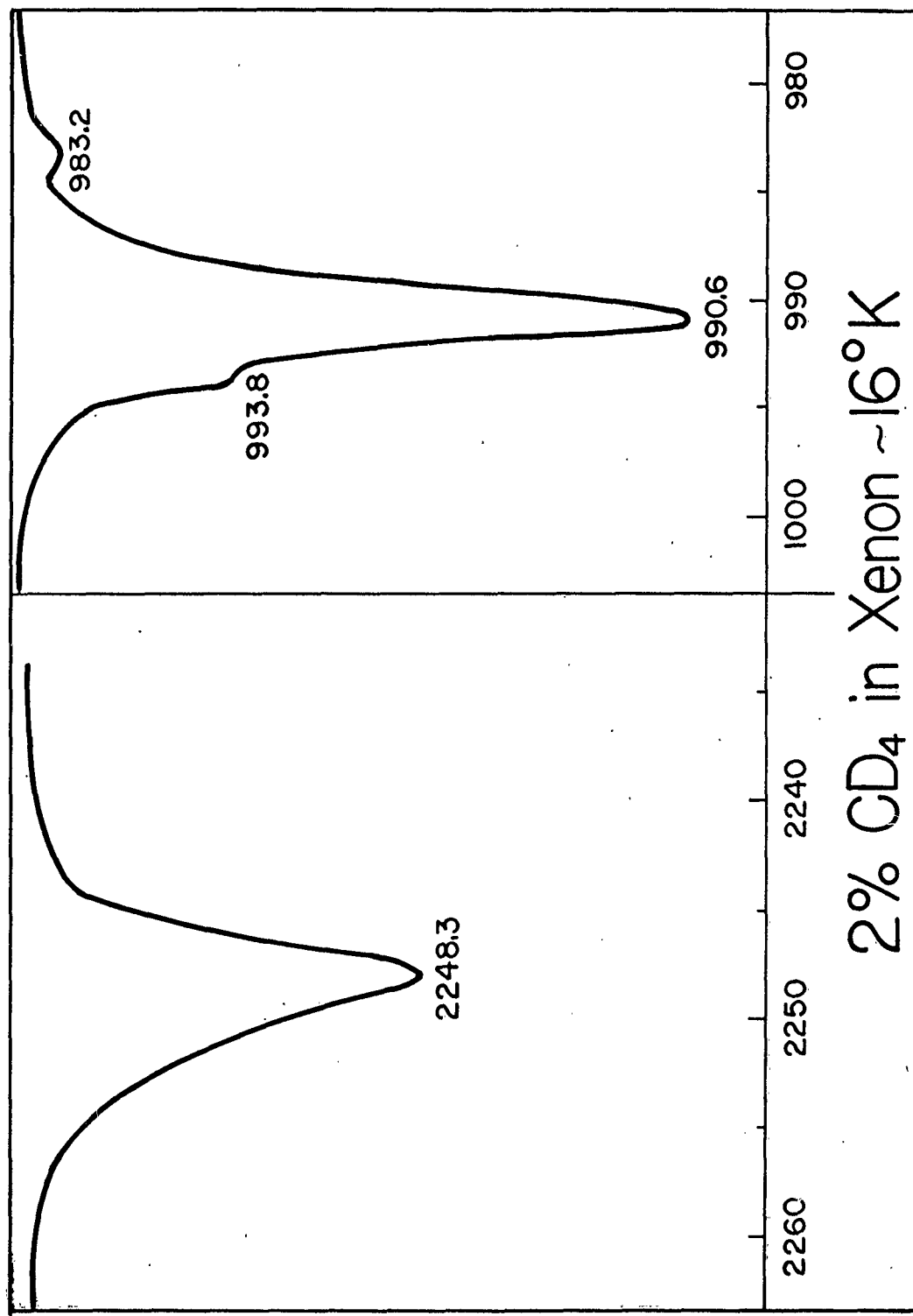


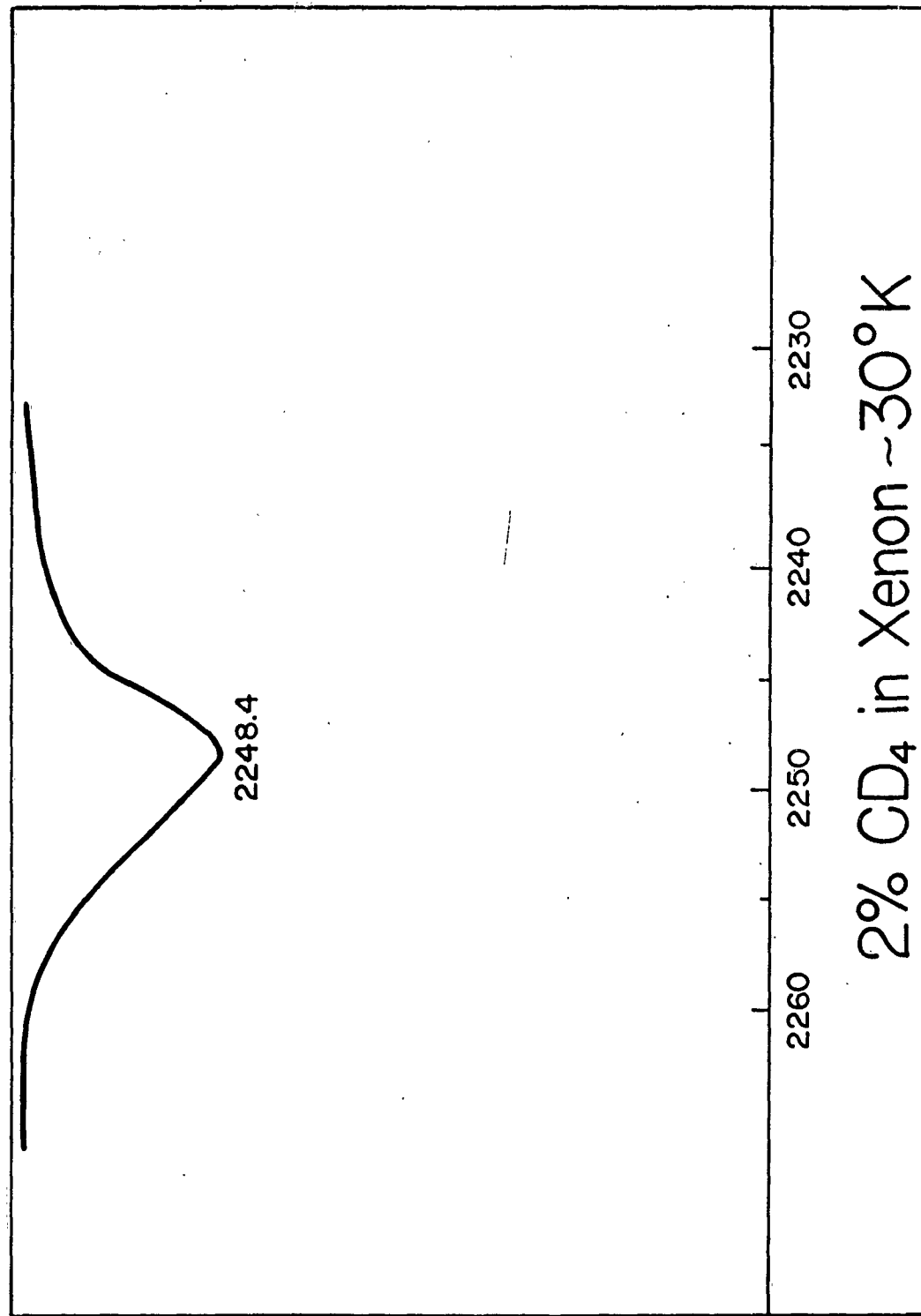


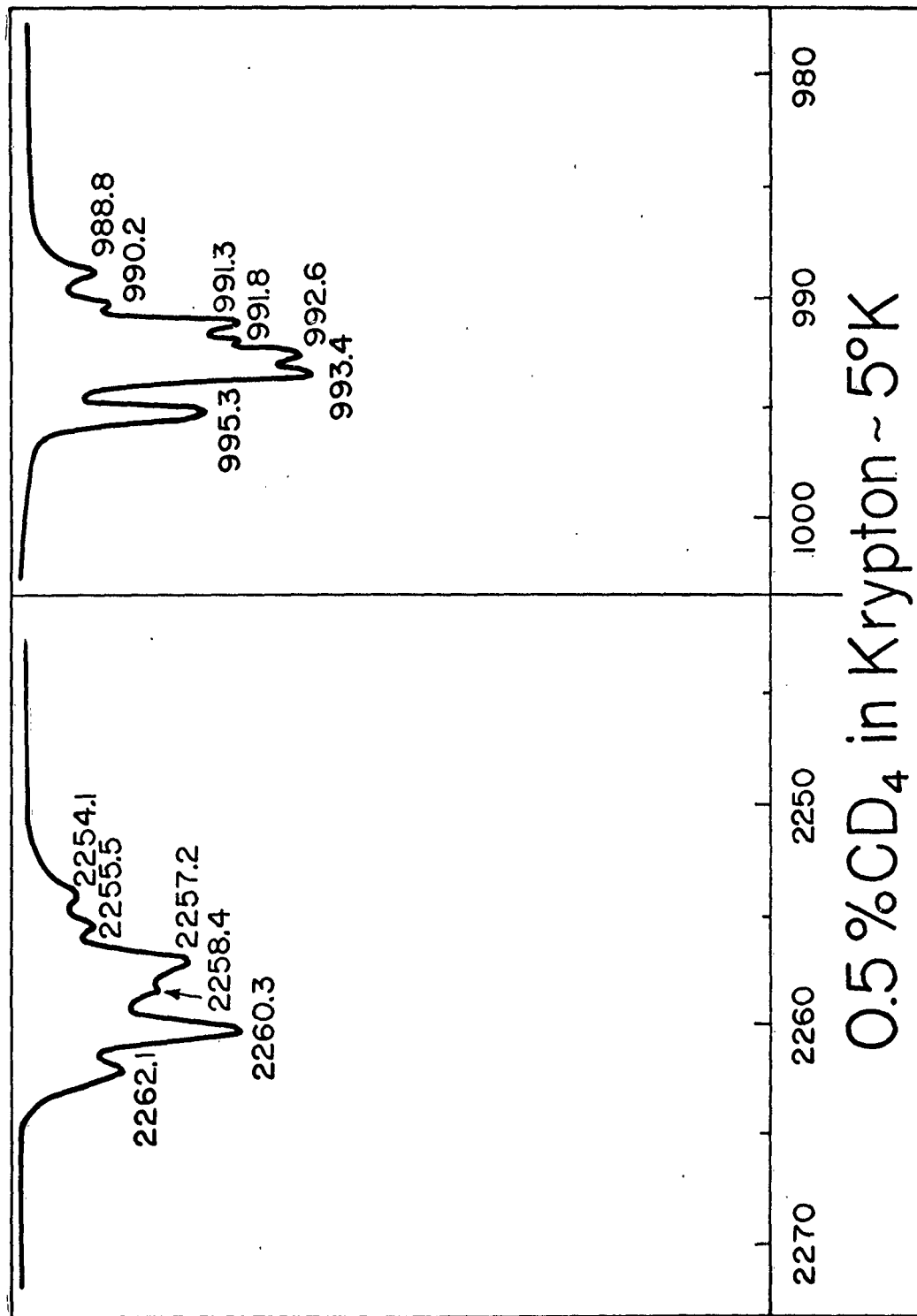


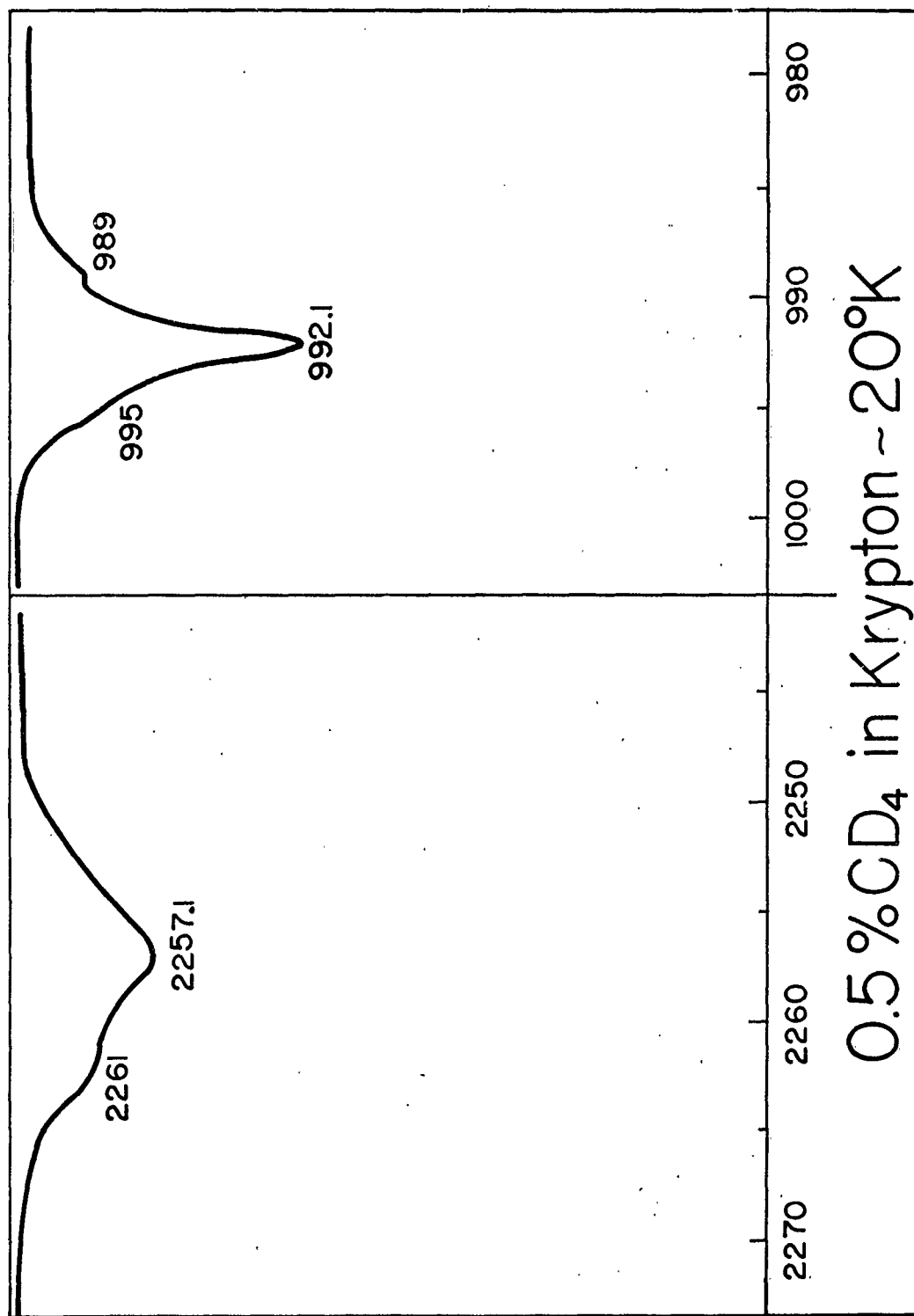


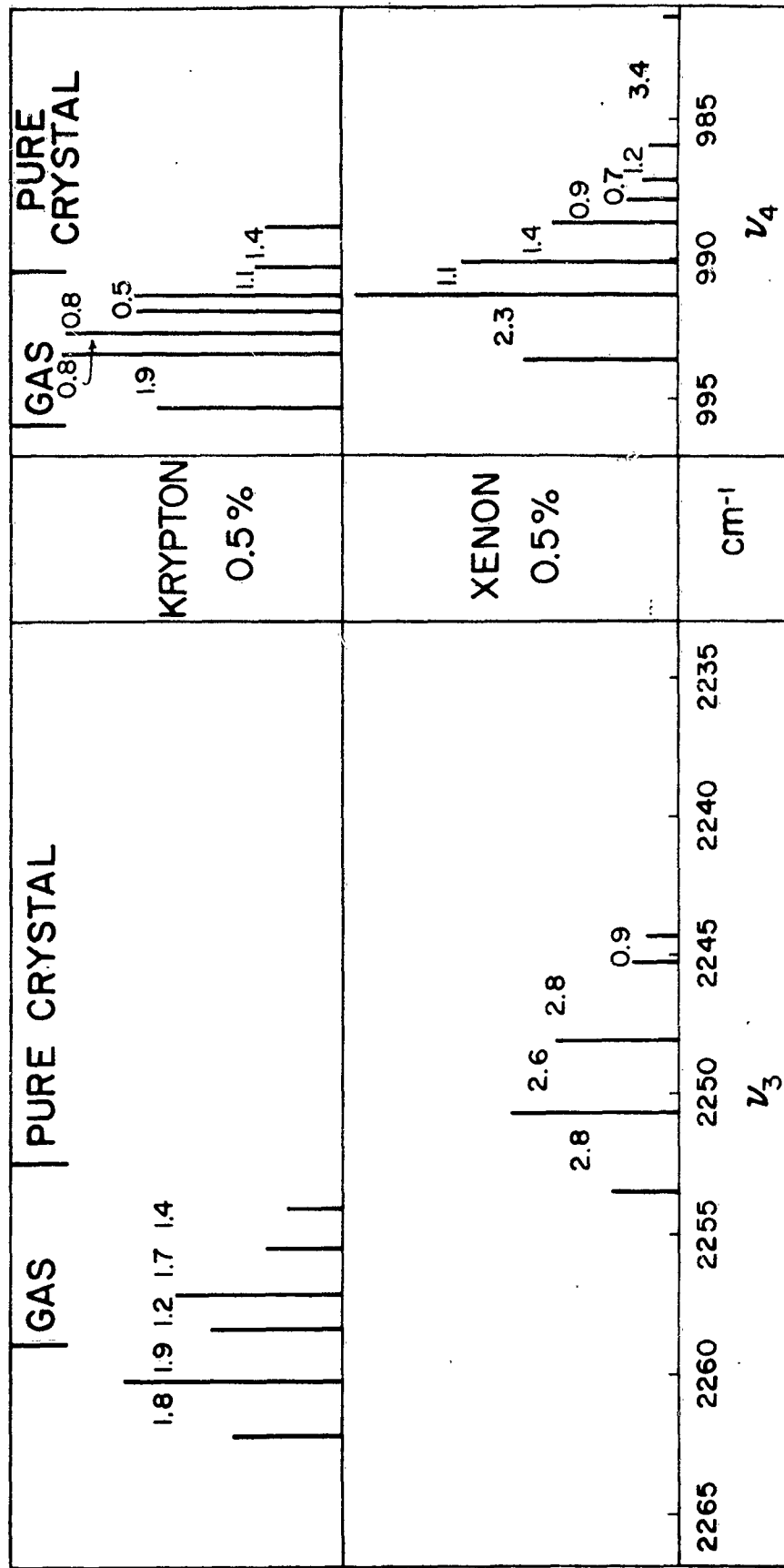






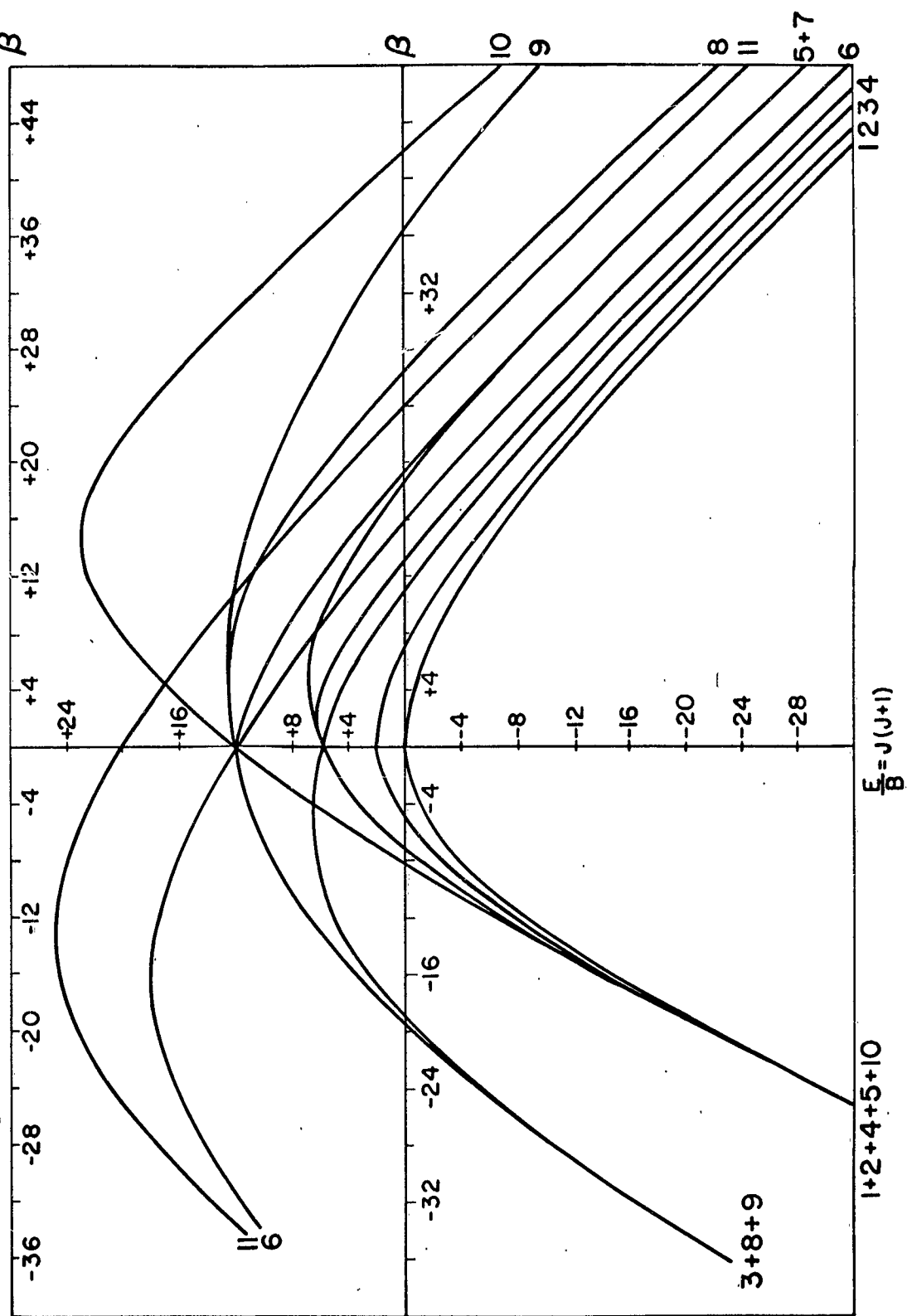


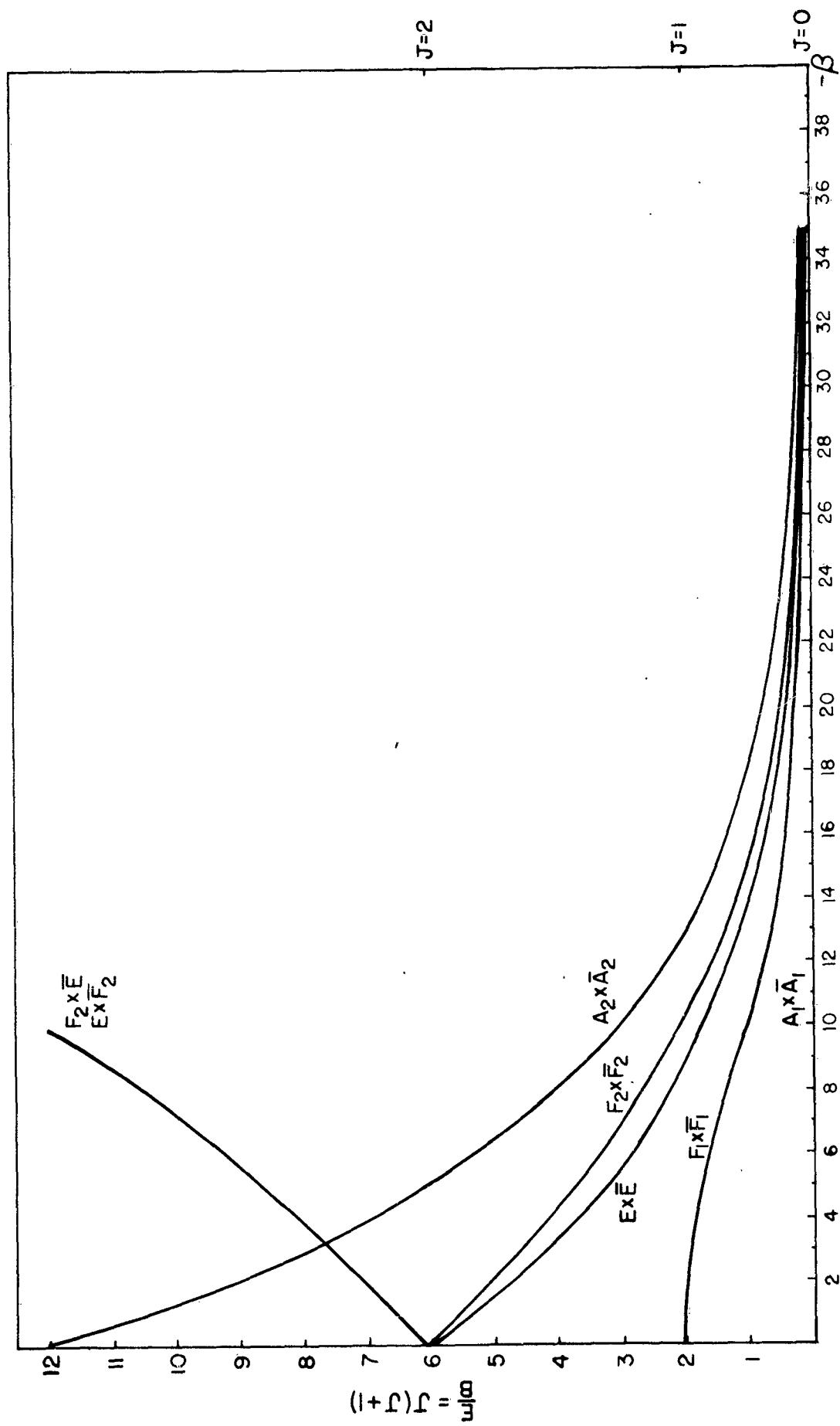


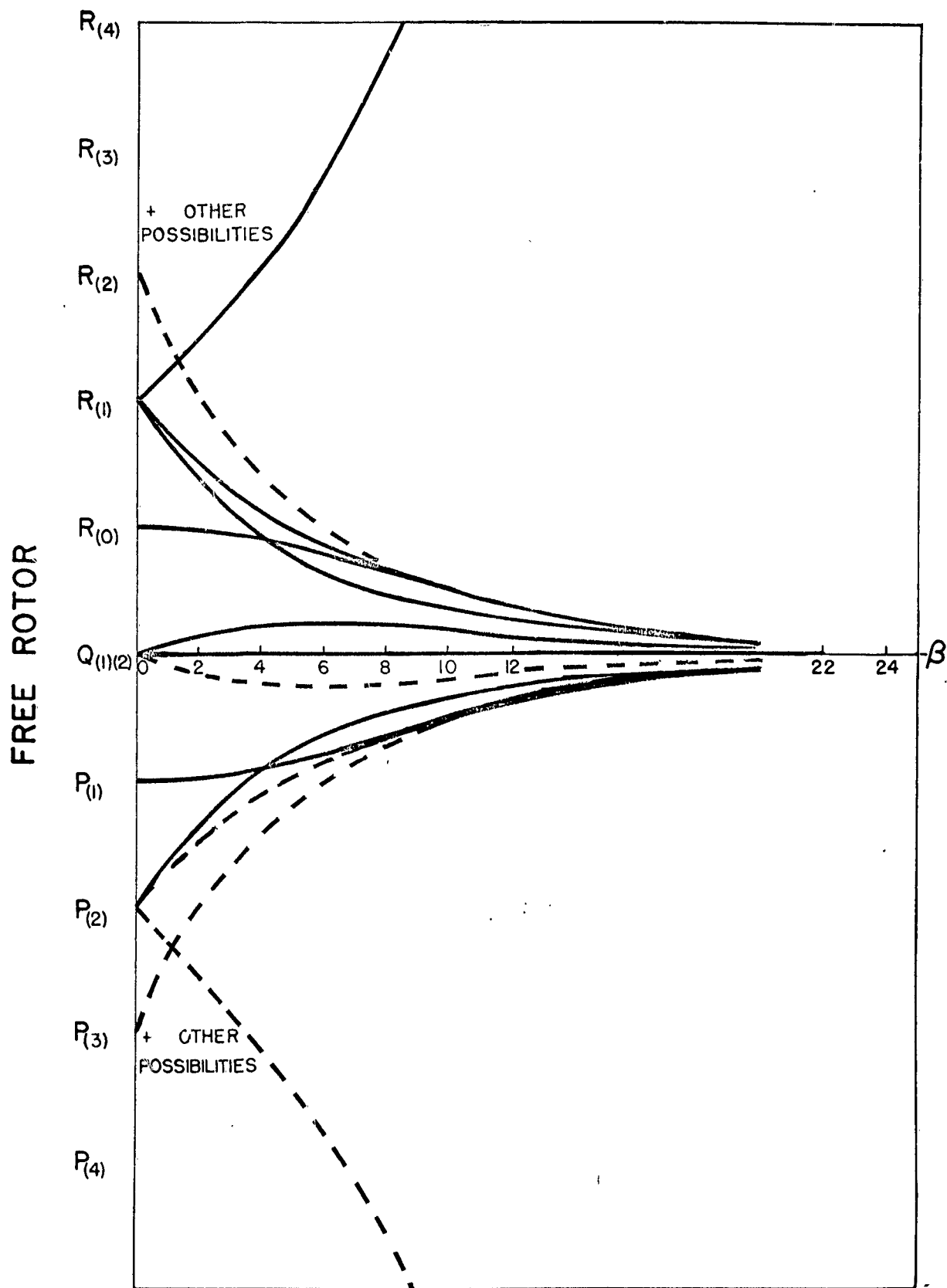


CD₄ IN SOLID SOLUTIONS

B







ROTATION-VIBRATION TRANSITIONS
OF KING'S HINDERED ROTOR